Aus der Medizinischen Klinik und Poliklinik II

Klinikum der Ludwig-Maximilians-Universität München

WNT1-inducible signaling protein-1 induced by TGF-β1 contributes to fibrosis in Crohn's disease

Dissertation
zum Erwerb des Doktorgrades der Humanbiologie
an der Medizinischen Fakultät der
Ludwig-Maximilians-Universität München

vorgelegt von

Shiqian Liu

aus

Linfen/Shanxi, China

Jahr

2023

Mit Genehmigung der Medizinischen
Fakultät der Ludwig-Maximilians-
Universität zu München

Erster Gutachter:	Prof. Dr. med. Helmut Friess
Zweiter Gutachter:	Prof. Dr. med. Julia Mayerle
Dritter Gutachter:	Prof. Dr. Koland Kappler
Mitbetreuung durch den promovierten Mitarbeiter:	PD Dr. med. Philipp-Alexander Nuemann
Dekan:	Prof. Dr. med. Thomas Gudermann

Tag der mündlichen Prüfung: 12.07.2023

Contents

Abstract

Background: Intestinal fibrosis is a common and serious complication of Crohn's disease (CD), oftentimes leading to intestinal obstruction and necessitating surgical intervention. The exact pathomechanisms are still incompletely understood, and no specific anti-fibrotic therapy for CD is currently available. Wnt-signaling components have been shown to play a significant role in fibrosis formation in other organs, however, their role in intestinal fibrosis formation is not fully known.

Methods: Wnt signaling-specific qPCR arrays were used to analyze 84 Wnt-mediated signal transduction genes in fibrotic and non-fibrotic surgical specimen of patients with stricturing CD. Primary fibroblasts from a fibrotic section and non-fibrotic section were isolated. Cell proliferation and migration were measured by Ki-67 staining and wound healing assays. Cells were treated with TGF-β1 and WISP-1 for qPCR and functional analysis.

Results: Several Wnt related genes were differentially expressed in fibrotic regions. A histopathological score showed a strong correlation between WISP-1 expression and fibrosis in fibrotic intestinal segments. Primary fibroblasts isolated from intestinal tissue of CD showed a significant difference in cell proliferation, migration, and ECM production between the fibrotic and control group. Stimulation of the cells with proinflammatory TGF-β1 induced the activation of Wnt signaling components and induced WISP-1 expression. The presence of WISP-1 induced migration but not proliferation of fibroblasts.

Conclusions: Our results show that WISP-1 expression was associated with fibrosis formation in CD. According to this, WISP-1 might be a potential therapeutic target for attenuation of intestinal fibrosis in CD.

List of figures

List of tables

List of abbreviations

A

ANG	angiotensin II
APC	adenomatous polyposis coli
α-SMA	alpha smooth muscle actin

B

BGF	basic fibroblast growth factor
BMPs	bone morphogenetic proteins
BSA	Bovine Serum Albumin

C

CCN	CYR61, CTGF, NOV protein family
CD	Crohn’s disease
cDNA	complementary DNA
CK1	casein kinase 1
cm	centimeter
CT	cysteine-knot-containing
CTE	Computed tomography enterography
CTGF	connective tissue growth factor
ctrl	control
CT-value	cycle of threshold value in quantitative PCR
CYR61	cysteine rich 61
℃	degree Celsius

D

d	day(s)
DAPI	4,6-diamidino-2-phenylindole
DKK2	Dickkopf homolog 2
DMSO	Dimethyl sulfoxide
DNA	dexyribonucleic acid

DVL	Disheveled

E

ECM	extracellular matrix
EDTA	ethylenediaminetetraacetic acid
EGFR/ERK	epidermal growth factor receptor/extracellular signal regulated kinase
EMT	Epithelial-mesenchymal transition

F

FAK	Focal adhesion kinase
FB	fibroblast(s)
FBS	Fetal Bovine Serum
FGS	Fibroblast Growth Supplement
FM	Fibroblast medium
Fz	Frizzled

G

g	gram, standard acceleration
GDFs	growth and differentiation factors
GI	gastrointestinal
GSK-3β	glycogen synthase kinase 3β

H

h	hour(s)
HCl	Hydrochloric acid
H&E	haematoxylin and eosin
HBSS	Hank’s balanced salt solution
HPIFs	human primary intestinal fibroblasts

I

IBD	Inflammatory bowel disease
IGF	insulin-like growth factors

IGFBP	insulin-like growth factor-binding protein
IgG	immunoglobulin protein G
IL	interleukin
IPF	idiopathic pulmonary fibrosis

L

l	liter
LAP	latency-associated peptide
IEF	lymphocyte enhancing factors
LOX	lysyl oxidase
LRP	Low-density lipoprotein receptor-related protein
LTBPs	latent TGF-β binding proteins

M

m	milli
M	molar
MMP	matrix metalloprotease
MRE	magnetic resonance enterography
mRNA	Messenger ribonucleic acid
MSCs	Mesenchymal Stem/Stromal Cells
MTT	3-(4,5-dimethylthiazol-2-yl)-2,5-diphenyltetrazolium bromide
µ	micro

N

n	nano
NaCl	Natriumchlorid
NOV	nephroblastoma overexpressed

O

OMUS	Obliterative muscularization of the submucosa

P

PBS	phosphate buffered saline

PBST	phosphate buffered saline with Tween 20
PCA	Principal component analysis
PCP	planar cell polarity
PCR	polymerase chain reaction
PDGF	platelet-derived growth factor
PFA	paraformaldehyde
PPARγ	Peroxisome proliferator-activated receptor γ

Q

qRT-PCR	quantitative real time PCR

R

rpm	revolutions per minute
RNA	ribonucleic acid

S

s	second
SEM	standard error of the mean
SFRP4	secreted Frizzled Receptor Protein 4
SD	standard deviation
SMCs	smooth muscle cells
SPARC	Secreted protein acidic and rich in cysteine

T

TBS	Tris Buffered Saline
TCF	T-cell factor
TGF	transforming growth factor
Th17	T helper 17
TIMP	tissue inhibitor of metalloproteinase
TLRs	toll-like receptors
TNF	tumor necrosis factor
TRAIL	TNF-related apoptosis-inducing ligand 1
Tris	tris(hydroxymethyl)-aminomethane
TSP	thrombospondin

U

U	unit
US	ultrasound

V

V	volt, volume
VEGF-A	vascular endothelial growth factor-A
VSMCs	vascular smooth muscle cells
VWC	von Willebrand factor type C

W

w	weight
WISP-1	WNT-inducible signaling pathway protein 1

Y

y	year

1. Introduction

1.1 Fibrosis in Crohn’s disease

Crohn's disease (CD) is an irreversible recurrent chronic inflammatory bowel disease (IBD) that affects all the gastrointestional tract. It can result in lesions ranging from the mouth to the anus, as well as extraintestinal disorders. The highest increase in incidence occurred in established high-prevalence populations with IBD in North America and Europe during the mid-20th century[1]. Furthermore, more than 30% of patients develop intestinal fibrosis, which can lead to problems such intestinal obstruction, perforation, and fistula[2]. The most common treatment for these patients is surgery or dilated with an endoscope to reduce their obstructive symptoms. Incidences of recurrence are high after surgery: 11–32% after 5 years, 20–44% after 10 years, and 46–55% after 20 years[3]. Despite the availability of older (anti-TNF-alpha antibodies) and novel biologics for the treatment of CD, no anti-fibrotic therapy to prevent or reverse intestinal fibrosis is now available[4].

1.1.1 Definition of fibrosis in CD

An accurate diagnosis is determined by examining the patient's medical history, assessing their symptoms, and taking objective measurements through endoscopy, imaging, and laboratory testing. CD should not be diagnosed or ruled out based on a single variable or outcome. The level of evidence and recommendation grade according Gastroenterologists' American College and the Organization for Crohn's and Colitis in Europe consensus guidelines are available as follows(Table 1)[5, 6].

Table 1 Typical features of CD

	Features
History	Smoking, family history, recent infectious gastroenteritis, etc.
Clinical features	Pain, diarrhea, exhaustion, and weight loss.
Examination	Abdominal pain and mass, extraintestinal manifestations including perianal abscess, and analfissure.
Laboratory	Inflammatory response, anaemia, malabsorption, CRP, and faecal calprotectin.
Endoscopy and Radiology	Skip lesions with patchy inflammation. Longitudinal ulcers (cobblestone, fistulous orifices, and stricture).
Histology	Granulomatous inflammation

In IBD, the Montreal and Paris classification provides aspects of clinical definition and classification (Table 2)[7].

Table 2 CD classification in Montreal and Paris

	Montreal	Paris
Age at diagnosis	A1: ≤ 16y	A1a: <10y A1b: 10-16y
	A2: 17- 40y	A2: 17- 40y
	A3: ≥ 40y	A3: >40y
Location	L1: ileal	L1: ileal
	L2: colon	L2: colon
	L3: ileocolonic	L3: ileocolonic
	L4: upper*	L4a: The disease is located in the area of the ligament of Treitz in the upper*
		L4b: The disease is proximal to

		one-third of the ileum and distal to the Treitz junction in the upper*
	B1: not encumbering or penetrating	B1: not encumbering or penetrating
Behaviour	B2: stricturing	B2: stricturing
	B3: penetrating**	B3: penetrating**
		B2B3: both penetrated and structural illness, either concurrently or sequentially
Growth	P: perianal disease modifier†	G0: No growth slowdown
		G1: Growth slowdown

* The use of L4 or L4a/L4b in conjunction with L1-L3 may be indicated in patients with concomitant upper gastrointestinal disease.

** This type of complication is defined as perforation, intraabdominal fistula, inflammation, and abscess occurring during the progression of the illness, and does not constitute an additional surgical complication (except for isolated perianal or rectovaginal fistulas).

† When a concurrent perianal ailment exists, the letter "p" is added to B1–B3.

The diagnosis of CD is not based on a single criterion. There are several tests that can confirm the diagnosis and determine severity and complications, including endoscopy, histology, radiology, and/or biochemistry. As one of complications of the disease CD fibrosis is characterized by intestinal obstruction. The most prevalent cause is terminal ileal stenosis for surgery in CD fibrosis patients, while strictures and fibrosis can develop anywhere in the digestive system. Stricture generation is a common component of CD's natural history.

Stiffness can be diagnosed with an endoscope or cross-sectional image technique. Endoscopy examination of a stricture has two advantages: it may simultaneously give treatment and gather anatomical tissue samples for investigation (Table 3). However, endoscopy with biopsies can’t tell how much fibrosis is in the intestinal tract since CD is a trans-mural disease characterized by inflammation and fibrosis. Nevertheless, an imaging technique based on cross-sections is suggested before endoscopic therapy to define the anatomy (position, number, dimension, morphology of strictures, and any concomitant problems that exclude the treatment of endoscopy)8. Intestinal ultrasound (US) computed tomography enterography (CTE), and magnetic resonance enterography (MRE) are among the most common

imaging technologies to detect CD-related strictures. For evaluating an obstruction in intestine or colon, the precision of all three imaging methods is high: CTE has a sensitivity of 89% and a specificity of 99% ; MRE has a sensitivity of 89% and a specificity of 94% ; and US has a 79% sensitivity and a 92% specificity[9].

Table 3 Crohn's Disease Endoscopic Score [10]

Variable	0	1	2	3
Ulcer size (cm)	None	Ulcers of the aphthous membrane (0.1 to 0.5 cm in diameter)	Ulcers with a diameter of 0.5-2 cm	Very large ulcers (diameter >2cm)
Ulcerated surface	None	Below 10%	10-30%	Over 30%
Affected surface	Segment not affected	Below 50%	50-75%	Over 75%
Narrowings present	None	One, is passable	Multiple, is passable	Unpassable

All the variables for the five bowel segments are added up to form a simple endoscopic score for CD. A variable is assigned a value for each segment of the bowel examined.

1.1.2 Pathological features of fibrosis in CD

Despite being poorly understood, stricturing CD is a complex pathogenesis that involves both inflammatory and non-inflammatory pathways in its development[11, 12]. While chronic inflammation may contribute to intestinal fibrosis, at least *in vitro* and in experimental animal models, it remains a key factor behind intestinal fibrosis expression patterns and fibrosis reduction through anti-inflammatory molecules[13-15]. The strictured wall histologically increased thickness by twofold due to a disproportionate amount alterations throughout each layer[16]. It is difficult to investigate the events leading up to the occurrence of strictures, since it is a slow, gradual process that only becomes evident later.

- Collagen changes and fibrosis

The extracellular matrix is made up of collagen, which is an important component. Homeostasis and repair of tissue damage depend on its production and deposition. Collagen is characterized either as an interstitial protein (type I, II, and III) or a protein of the basal lamina (type IV). The overexpression of this collagen subtype in the gut of CD patients produces extracellular matrix (ECM) that is conducive to scar contraction and stricture formation. The fibroblast, myofibroblast and SMC are the three cell types that secret collagen within the intestinal wall.

Strictures are caused by prolonged dysfunctional repair mechanism and inflammation across the membrane, leading in an excess of ECM synthesis and deposition in the intestinal wall[17]. Detected in strictures are collections of mesenchymal cells and modifications in their behavior caused by changes in histology. A variety of mesenchymal cells are found in the tissue, including fibroblasts, myofibroblasts, and smooth muscle cells, which are key mediators in the formation of strictures, and the increasing number of mesenchymal cells combined with excessive ECM secretion is considered a hall mark of strictures[18]. An important component of the fibrosis caused by CD is the presence of fibroblasts. Proliferation, migration, and ECM secretion are all enhanced in intestinal tissue with fibroblast activation, which is the primary feature of intestinal fibrosis[19]. Fibroblasts are induced to undergo fibrosis by several cytokines and chemokines. In terms of profibrotic agents, transforming growth factor- β1 (TGFβ1) is the most effective. A TGF-β1 treatment increases the migration of fibroblasts in a normal environment. Fibrosis occurs due to an out of balance deposition and degradation of the ECM in IBD. There is an increase in the activity of matrix metalloproteinases (MMPs) in CD intestinal tissue, and MMP-1, 2, 3, and 9 play a significant role in the degradation of the ECM[20]. It has been shown that tissue inhibitors of metalloproteinases (TIMPs) interfere with active metalloproteinases by noncovalently binding to its active form. When TIMPs and metalloproteinases are imbalanced, excessive ECM deposition and tissue fibrosis may occur[21].

Intestinal myofibroblasts, also known as intestinal stromal cells, are generated in adults from intestine mesenchymal stem cells that are supplemented by mesenchymal stem cells and stromal cells derived from bone marrow after severe intestinal injury[22]. When stimulated with various mediators, fibroblasts tend to transform into myofibroblasts in the absence of α-SMA.[23]. A subepithelial location

of myofibroblasts is present within the intestinal mucosa, which allows them to exhibit larger contractile forces than fibroblasts. Myofibroblasts, once triggered, can produce large amounts of ECM and so cause fibrosis in the gut[24]. Several mediators from different classes are capable of activating myofibroblasts, including inflammatory mediators (TNF-α, IL-13, IL-36, and IL-1), peroxisome proliferator activator receptors, growth factors (TGF-β1, epidermal growth factor, platelet-derived growth factor [PDGF], connective tissue growth factors, insulin-like growth factors [IGF]-1 and 2, and basic fibroblast growth factors), stem cell factor, endothelins I, II, III, and angiotensin II (ANG II)[25-27]. Furthermore, activated myofibroblasts express lysyl oxidase (LOX), which can crosslink collagen and cause contractions of the extracellular matrix[24].

Smooth muscle cells (SMCs) (α-SMA positive and desmin positive) can be located in the muscularis mucosa, muscularis propria, and surrounding arteries in the intestinal wall. Intestinal myofibroblasts and SMCs are in a dynamic balance. SMCs can transdifferentiate into myofibroblasts in the presence of persistent inflammation[26]. IL-6 production increases stimulated by TGF-β and IL-1β, therefore contributing to intestinal inflammation[28]. Intestinal SMCs contribute to thickening and strictures in the intestinal wall by undergoing fibrous hyperplasia and obstruction of the submucosa[11, 29].

- Smooth muscle pathology

CD is characterized by the spread and hypertrophy of the mucosal muscularity and the disorganization and splaying of the muscularis propria. In around 1/3 small intestine samples from resections of CD, a structural disorder is characterized by obliterative muscularization of the submucosa (OMUS)[29]. In CD, the number of SMCs in the intestine increases. Not only is the muscularis mucosae thickened all over, but it should also be noted, enormous muscle cells arranged in a characteristic, irregular pattern. Therefore, CD in the intestine is typically detected pathologically as alterations in the smooth muscles and submucosa, which result from the overall alterations therein.

In summary, CD strictures is a constantly changing process in which mediators, cell populations, and physical conditions change.

- Fat pathology in CD

A thicker mesentery with adipose tissue overgrowth is visible under the microscope. Fat-wrapping is characterized as white adipose tissue expansion from the

mesenteric attachment to partially or completely cover the antimesenteric section of the intestine. It is one of the characteristics of CD[30, 31]. Fat-wrapping was linked to transmural inflammation in the form of lymphoid aggregates, and there were also links found between fat-wrapping and other connective tissue modifications such as fibrosis, muscularization, and stricture development.

1.1.3 Pathomechanisms of fibrosis in CD

CD is a feature of chronic inflammation, ulcers, and intestinal damage, which results in recurring attempts to heal and close the gap between ulcers via disorderly ECM. In addition to the mucosa, the submucosa, the muscularis propria, and the serosa, the gut wall can be affected by fibrosis due to CD's transmural inflammation. Fibrosis cannot be reversed due to chronic inflammation. CD-associated strictures undergo resection at a high rate of inflammation and fibrosis, which are highly correlated in severity[32]. IL-17A, IL-22 and IL-21 are secreted by T helper 17 (Th17) cells, and they may have a significant impact on inflammation and fibrosis associated with CD[33, 34]. Patients with active CD and strictures have increased levels of IL-17A in their mucosa and lamina propria[35-37]. IL-17A receptors are upregulated in myofibroblasts, which reduces their migration abilities, as well as producing more ECM and expressing MMP-1 inhibitors[37]. Besides Th17 cells, Th2 immune cells are also important for fibrosis and wound healing. Cells of the Th2 type produce cytokines such as IL-13, IL-9, IL-4, and IL-5, among which IL-13 is known for one of the most powerful mediators of fibrogenicity[38, 39]. A strictured CD intestinal tissue produces IL-13 that leads to the deposition of ECM through an increase in TGF-β secretion[40, 41]. Experiments with experimental colitis show that IL-4 and IL-13 levels increase in chronic inflammation, particularly at the end [42]. This results in an immunophenotype dominated by Th1, while one dominated by Th2 in late CD. In the process of repair, regeneration, and fibrosis of tissues, macrophages may play a crucial role[43, 44]. Research has shown that macrophages produce IL-10, cytokine that inhibits inflammation by limiting fibroblast collagen production induced by TGF-β[45]. It was demonstrated that STAT6 deficiency increased $CD16^{+}$ macrophages and contributed to intestinal fibrosis in animal models[43]. As a result, immune cells stimulate mesenchymal cells to fibrosis by

secreting cytokines. Intestinal strictures have not been prevented or treated by suppressing inflammation to date. Intestinal fibrosis is likely triggered by inflammation but targeting inflammation has not been shown to be a significant prevention or treatment[11]. The presence of adhesion molecules such as integrins and cadherins is an independent driver of inflammation-induced fibrosis. It has been proven that molecules targeting them are effective in treating fibrotic disease elsewhere. IBD strictures may be treated with this approach in conjunction with anti-inflammatory therapy[18]. As well, the imbalance of the microbiota in CD patients and the activation of toll-like receptors (TLRs) contribute to CD fibrosis[46, 47]. Fibrosis associated with CD is caused by the activation of TLRs[48]. The reduction of CD stenosis may be achieved by blocking specific TLRs on selective bacteria components.

As a consequence of this damage, the transmural membrane thickens and stiffens, as well as the intestinal lumen narrows, which can lead to strictures and blockages. A greater number of myofibroblasts and activated fibroblasts deposit types I, III, and V of collagen in submucosal gaps and muscle layers, forming the ECM[49]. In the latter, mesenchymal cells multiply, epithelial-to-mesenchymal or ectomesenchymal transitions are initiated, or fibrocytes derived from bone marrow are recruited and differentiated[50-52]. Transforming growth factor-1 (TGF1) is responsible for the development of fibrosis, but numerous growth factors and cytokines also contribute to its pathophysiology. A few of them are interleukin (IL)-4, IL-5, IL-13, platelet-derived growth factor (PDGF), connective tissue growth factor (CTGF), basic fibroblast growth factor (BGF) and insulin-like growth factor (IGF) that regulate bone morphogenesis[53]. TGF-β1 is involved in fibroblast recruitment, transdifferentiation to myofibroblasts, and ECM secretion stimulation[54, 55]. It promotes wound healing by preventing inflammation as well as causing fibrosis through its antiinflammation properties. The amount of ECM protein synthesis and breakdown determine the depth of fibrosis.

1.2 WNT1-inducible-signaling pathway protein 1

WNT-1 inducible signaling pathway protein 1 (WISP-1), alternatively identified as CCN4 or Elm1, is a protein with a high cysteine content that belongs to the CCN

family in mammalian cells[56, 57]. Matricellular proteins are a subset of ECM proteins that modulate cellular responses like cell proliferation, differentiation, and survival but have no structural function[58]. The mouse WISP-1 homologue was discovered by comparing the expression levels in low and high metastatic cells, and was dubbed “expressed in low metastatic cells” as a result(Elm1)[56]. Human WISP-1 was discovered in 1998 as a WNT1-induced gene in the mammary epithelial cell line C57MG overexpressing WNT1[59].

WISP-1 is a member of the CCN protein family. The CCN acronym is named after the first three members of the CCN family: cysteine rich 61(CYR61/CCN1), connective tissue growth factor (CTGF/CCN2), and nephroblastoma overexpressed (NOV/CCN3). Pennica et al. (1998) identified three WISP proteins (WISP1-WISP3), which were all assigned to the CCN family in 2003 and renamed CCN4/WISP-1, CCN5/WISP-2, CCN6/WISP-3[60].

1.2.1 WISP-1 gene and protein structure

WISP-1 is a gene located on human chromosome 8q24.1 to 8q24.3 that contains five exons and four introns and the cDNA length is 1,766bp and 2,830bp, respectively (NCBI Gene ID 8840). WISP-1 encodes 367 amino acids, including 38 conserved cysteine residues and four possible N-linked glycosylation sites (84 percent identical to the murine version). The protein encoded by the WISP-1 gene has a projected relative molecular mass of 40 kD[59, 61]. WISP-1 and WISP-3 are the most comparable (42 percent similarity), whereas WISP-2 is 37 percent identical to WISP-1, according to an alignment of the three human WISP proteins[62]. Modules found in WISP proteins are similar to those found in members of the CCN family, which consists of four cysteine-rich domains that are all conserved and distinct. IGFBP (insulin-like growth factor binding protein-like module), VWC (von Willebrand factor type C repeat), TSP1 (thrombospondin-homology type 1 repeat), and CT (C-terminal cysteine-knot-containing) domain are the four structural domains(Figure1)[57]. These domains work in tandem as well as independently. The first twelve cysteine residues of the N-terminal domain contain a GCGCCXXC consensus motif that is preserved in nearly all insulin-like growth factor-binding proteins (IGFBPs). The following ten cysteine residues are covered by the von VWC module, which is hypothesized to be involved in protein complex formation

and oligomerization63. MMPs are especially vulnerable to proteolytic degradation of a brief variable region next to the VWC domain64. Six cysteine residues and an unique WSXCSXXCG motif are found in the TSP domain, the third area, which is involved in connecting sulfated glyco conjugates65. With the exception of WISP-2, all members of the CCN family possess a C-terminal cysteine knot-like (CT) domain that is connected to receptor binding and dimerization66.

A CCN family member consists of four cysteine-rich modules that are preserved, and it's been suggested that missing more than one of them causes splicing variations or gene mutations. Furthermore, WISP-1/CCN4 transcripts are expected to be completed, three variations have been found (1,204 bp). Among the variations was WISP-1v (short for VWC module II). VWC is encoded by a 260-nucleotide exon3 that is absent in this variant's 840-nucleotide mRNA species67. The IGFBP domain of WISP-1vx is shorter than its entire length since a frame shift resulted in the fusion of IGFBP and CT domains. IGFBP module contains a unique C-terminal amino acid substitution, and two hepatocellular carcinoma cell lines exhibit this mutation68. WISP-1 Eex3–4 has a splice mutation that leads in a shortened transcript length of 750 nucleotides, as well as a shift of frame in 2 and 5 exons that causes prematurely ending. This mutation was found in a chondrocytic cell line , and the predicted protein only contains the first module 69.

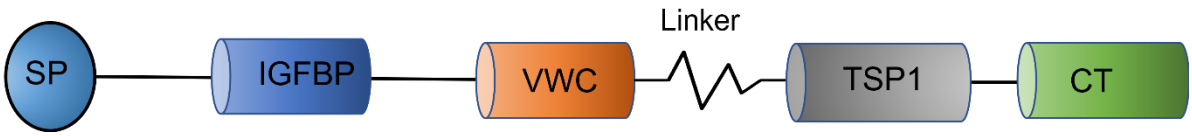

Figure 1. Schematic structure of WISP-1 proteins. It is made up four protein modules (IGFBP, VWC, TSP1 and CT) and possess one N-terminal secretory signal peptide. SP: signal peptide, IGFBP: insulin growth factor binding protein, VWC: van Willebrand Factor C, TSP1: thrombospondin type 1 repeat, CT: C-terminal domain (Figure created with power point).

1.2.2 WISP-1 expression

During development, WISP-1 expression has been detected, particularly in the bones and intestinal disease. WISP-1 is an osteogenic potentiating factor that encourages mesenchymal cell proliferation and osteoblast development while inhibiting chondrocytic differentiation. WISP-1, as a result, plays a critical regulatory

role in bone formation and fracture repair[70]. Chao et al. also showed evidence that WISP-1 is linked to osteoarthritis by encouraging changes in bone structure[71, 72]. In the gut, WISP-1 mRNA and protein expression were elevated in IBD patients' colonic samples compared to healthy controls[73].

A variety of human tissues express WISP-1, including the liver, kidneys, lungs, pancreas, placenta, and small intestine[74-81]. The brain, liver, skeletal muscle, colon, peripheral blood leukocytes, prostate, testis, and thymus all showed little or no expression.

WISP-1 expression in different human organ cancers varies in severity. On the whole, WISP-1 expression has been linked to tumor progression, and elevated WISP-1 expression has been seen in tumor tissue compared to healthy organs tissue in a variety of tumor forms (Breast cancer, Gastric Adenocarcinoma, Pancreatic cancer, Head and Neck cancer, Lung adenocarcinoma, Colorectal cancer, etc.)[82-87]. Moreover, WISP-1 correlates with poor prognosis in the vast majority of cancer in incidences[88].

WISP-1 has been implicated in a wide variety of fibrotic disorders. In the lung fibrosis, WISP-1 has been discovered to be elevated in fibrosis of the lungs. In both experimental and human idiopathic pulmonary fibrosis(IPF), its expression is primary restricted to the alveolar epithelium[76, 89]. Similarly, WISP-1 expression is upregulated in the kidneys of animals with renal fibrosis[90]. WISP-1 was upregulated in both *in vitro* and *in vivo* liver fibrosis models, and WISP-1 induced hepatic stellate cells proliferation *in vitro*[91]. Overall, WISP-1 expression profiles point to a key role in fibrosis formation, as well as a strong link between WISP-1 and tissue remodeling mechanisms.

1.2.3 WISP-1 function and regulation

WISP-1 expression has primarily been linked to development and disease by influencing a variety of cell types in proliferation, invasion, migration, adhesion, ECM expression, survival/ apoptosis, differentiation, and metastasis.

WISP-1 is a member of the CCN growth factor family and is involved in the proliferation of cells. The transcription factor WISP-1 is induced by the proinflammatory cytokine tumor necrosis factor-alpha (TNF-α) in post-infarct hearts, stimulates cardiac fibroblast proliferation, and activates cardiovascular

regeneration[74]. In addition to cardiac fibroblasts, in primary human lung fibroblasts WISP-1 also increase IL-6 production, which enhance fibroblast proliferation[92]. Additionally, WISP-1 activates FAK (Focal adhesion kinase), which may then trigger the expression of vascular endothelial growth factor-A(VEGF-A) by stimulated epidermal growth factor receptor (EGFR) and extracellular signal-regulated kinase (ERK), and thereby promote the proliferation (Figure 2). Furthermore, WISP-1 may also play a key role in tumor cell invasion by activating the receptor αvβ3 that can then promote Ras/Raf/MEK/ERK, ASK-1, and FAK expression resulting in tumor cell invasion (Figure 2). A tumor cell overexpressing WISP-1 induces invasion, which appears to be a key event in the local restructuring process of the extracellular matrix or in the reorganization of loose collagen fibers generated by proteolytic cleavage of the extracellular matrix that is accompanied by tumor cell invasion[93]. Migration occurs through stepwise mechanical and chemical interactions between the cell and its surrounding environment. WISP-1 plays an important role in the migration of vascular smooth muscle cells (VSMCs)[94]. The WISP-1 protein increases osteosarcoma cell motility by upregulating MMP-2 and MMP-9 expression via the integrin receptor, Ras, Raf-1, MEK, ERK, and NF-κB pathways[95]. CCN family members have been reported to induce cell-matrix adhesion in multiple ways. For fibroblast adhesion function, WISP-1 facilitates cell-matrix adhesion in epithelial cells and the release of pro-angiogenic chemokines in fibroblasts by activating the β-catenin signaling pathway. It is WISP-1 whose C-terminal domains mediate cell to matrix adhesion[96]. It is well known that Wnt signaling is responsible for phosphorylating and inactivating constitutively active glycogen synthase kinase 3β (GSK3β). Thus, β-catenin does not undergo phosphorylation. In the nucleus, stabilized cytosolic β-catenin forms a complex with T-cell factor/lymphocyte enhancing factors (TCF/LEF) transcription factors, activating the transcription of target genes such as cyclin D1, c-Myc, and WISP-1, which are oncogenes and promote cell survival[97]. Some studies showed that WISP-1 plays an active role in human mesenchymal stromal cells derived from bone marrow. Death receptors and the ligand TNF-related apoptosis-inducing ligand 1 (TRAIL) are inhibited by WISP-1, while depletion of WISP-1 stimulates their expression and facilitates spontaneous cell death[98]. WISP-1 has shown to reduce death rates in patients with glioblastoma and colon cancer compared to those expressing higher levels of WISP-1[99, 100]. In terms of differentiation, WISP-1

inhibits the transcription of Peroxisome proliferator-activated receptor γ (PPARγ), one of the most important transcription factors in fat cell differentiation[101, 102]. In contrast, WISP-1 may play an active role in the differentiation of MSCs (Mesenchymal Stem/Stromal Cells). As we all known, the linearization of collagen is indicative of aggressive tumors and is a cause of metastasis. WISP-1 stimulates type I collagen linearization and enhances breast cancer metastasis without having any effect on gene expression[93].

In addition to altering cell behavior, WISP-1 also regulates wound healing and ECM production. WISP-1 treatment of human adult dermal fibroblasts indicated that it neutralized TNF-α induced suppression of col1a1 and fibronectin mRNA expression as well as TNF-α induced promotion of MMP-1 and MMP-3 mRNA expression[103]. WISP-1 interferes with the expression of multiple ECM proteins including TGFB1 (TGF-β induced), IGFBPs (insulin-like growth factor binding proteins), NOV (nephroblastoma overexpressed gene), and DKK2 (Dickkopf homolog 2). Moreover, these genes were profoundly reduced by WISP-1 knockdown. Therefore, WISP-1 contributes to the regulation of ECM genes in fibroblasts [104].

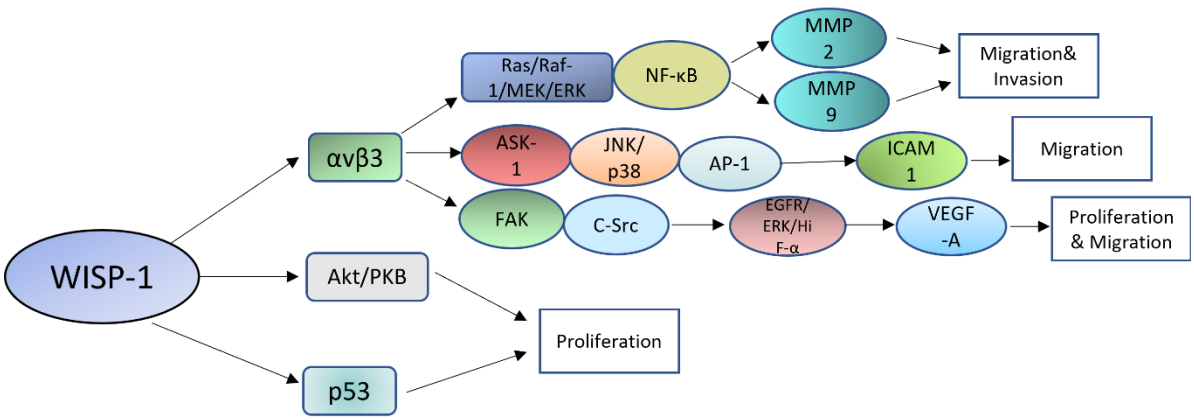

Figure 2. The cell signaling pathways involved in WISP-1 affect cell proliferation, migration, and invasion by activating Ras/Raf-1, JNK/p38, EGFR/ERK, Akt/PKB, p53 signaling pathway. (Image adapted from Feng. M. Chin J Cancer Res 28, 2016([62]))

Up to date, studies have shown that WISP-1 protein promotes wound healing in the intestinal epithelium[80], but no further elucidated it´s role during intestinal fibrosis formation, especially in CD.

1.3 Transforming growth factor beta 1

One of the most critical questions is what causes fibrosis in CD patients. The key event in the pathophysiology of CD is the generation of inflammatory cytokines. Among them, TGF-β1 activates the accumulations of collagen during wound repair in many organs including CD.

1.3.1 TGF-β1

TGF-β1 is considered the prototype of a large family of secreted, dimeric growth factors and cytokines encoded by 33 genes in humans and mice[105]. Human TGF family members include TGF-1, TGF-2, and TGF-3, activins, nodal proteins, bone morphogenetic proteins (BMPs), and growth and differentiation factors (GDFs). Additionally, other heterodimeric mixtures of these have been discovered and described as physiologically active proteins, despite being mostly studied as homodimers[106]. Further, signals induced by a non-compliant stroma can disrupt the latency constraints governing TGF-β1, resulting in the dimerization of TGF-β1, which can bind its receptor complex and promote myofibroblast differentiation or retention[107]. Several cell types produce TGF-1, including lymphocytes, macrophages, epithelial cells, and fibroblasts[108, 109](Figure 3). Secreted TGF-β1 interacts with the latency-associated peptide (LAP) to become inactive[110]. TGF-β1 becomes active when it is released from the LAP, dissociated from latent TGF-β binding proteins (LTBPs), and activated by plasmin, reactive oxygen species, thrombospondin-1, and acid (Figure 3). The protein is anchored in the ECM[111, 112]. Therefore, TGF-β1 has been considered one of the most significant ECM regulators.

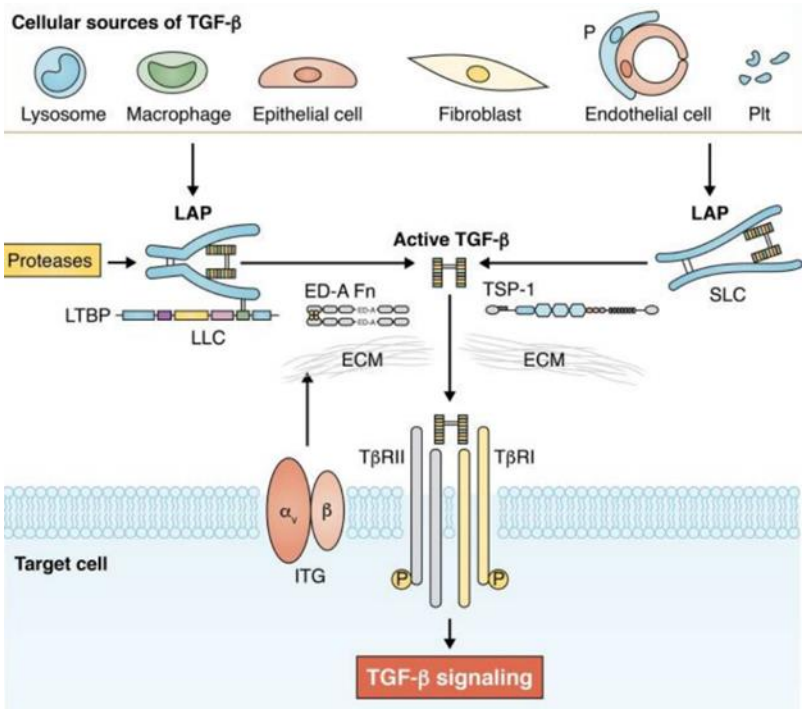

Figure 3. Expression and stimulation of TGF-β in fibrotic tissue. A variety of cell types can generate or release TGF-β at sites of injury. (Adapted from Nikolaos G. Journal of Experimental Medicine.217,2020[108])

1.3.2 TGF-β1 target regulation and function

Natural wound healing is a complex process that includes (1) cell inflammation and migration, (2) fibroblast proliferation leading to the development of granular tissue and the deposition of ECM, and (3) long-term remodeling of injured tissue.[106]. Multiple cell types have been shown to be affected by TGF-βs, regulating these different steps and promoting wound healing *in vivo*. TGF-β1 accelerates wound healing, as shown in early studies, initiated soon after TGF-β1 was isolated and purified[106]. TGF-β1 regulates inflammation, immune response, tissue repair, angiogenesis, and fibrosis. Among its many uses, TGF-β1 is also regarded as an inflammatory cytokine. TGF-β and IL-6 together stimulates Th17 cells to differentiate, which can result in further inflammation and autoimmune diseases[113]. Moreover, when combined with IL-4, TGF-β promotes the differentiation of IL-9- and IL-10-producing T cells, which lack suppressive functions and are associated with tissue inflammation[114, 115]. During intestinal immunity, TGF-β inhibits inflammatory responses and triggers immune tolerance to luminal bacterial antigens[115, 116]. The lamina propria of normal guts contains more TGF-β transcripts than the epithelium[117]. TGF-β1 is believed to be one of the most

important fibrogenic and growth-promoting cytokines in many organs that contribute to wound healing.

1.3.3 TGF-β1 and Wnt-signaling in CD fibrosis

As a result of TGF-1 stimulation, fibrosis involves the activation of a fibrotic response in a variety of cell types, such as macrophage, epithelial cells, and fibroblasts. As a regulator of fibrotic responses, macrophages release growth factors, cytokines, and matricellular proteins regulate fibroblast function and differentiation influence ECM remodeling[44]. TGF-β stimulates macrophages, resulting in reduced H_2O_2 release[118] and attenuated expression of proinflammatory genes[119]. A macrophage-produced secreted protein acidic and rich in cysteine (SPARC), which increases the rigidity of myocardium by enhancing the maturation of procollagen, is one of the matricellular proteins that increase rigidity[120]. Regarding the epithelial cell fibrosis, it enhances fibrogenicity in epithelial cells by directly or indirectly stimulating epithelial-to-mesenchymal transitions (EMTs)or indirectly by stimulating differentiation to myofibroblasts[121]. TGF-β may therefore cause tissue fibrosis in tissues with a large number of epithelial cells. Several experimental studies have demonstrated the role of TGF-β1 in fibrosis pathogenesis in many different tissues. TGF-β1 causes fibrosis associated with synthesis of extracellular matrix in different organs including kidney, liver, and lung and EMT[122-124]. Nevertheless, a key mediator of fibrosis, TGF-β1 promotes the production of extracellular matrix and the proliferation of myofibroblasts and fibroblasts[125]. In the mouse model, myocardial fibrosis is reduced when TGF-β signaling is deleted[126]. Also, TGF-β1 inhibitor prevents human tumor and lung fibrosis by inhibiting TGF-β1 signaling[127]. Renal fibrosis is associated with myofibroblasts, and recent studies have shown that macrophages recruited from bone marrow can transform into myofibroblasts in injured kidneys[128]. Fibrosis occurs when abnormal fibroblast activation leads to increased production and contraction of collagen-rich extracellular matrix[129]. TGF-β1 can cause fibrosis through related signaling pathways. There are two types of signaling pathways associated with TGF-β canonical and non-canonical (Figure 4). It is SMAD-dependent and acts via the transmembrane serine/threonine kinases TGF-β1 type

II (TbRII) and type I (ALK5) receptors. Through binding of TGF-β1, ALK5 recruits and associates with TbRII. Phosphorylation of SMAD2 and SMAD3 caused the formation of the SMAD2/3 complex, which recruits SMAD4. Thus, SMAD2/3/4 will act as transcription factors that promote the expression of pro-fibrotic genes (ECM genes, including collagen genes COL1AL1, COL3A1, TIMP1, and other ECM-related genes)130. ALK1, another TGF-β type I receptor, is involved in non-canonical SMAD-dependent TGFβ1 signaling. ALK1 is joined by TGF-1, and ALK1 then attracts and interacts with ALK5. TGF-β1 binds ALK1, which in turn recruits and associates with ALK5. Before recruiting SMAD4, the newly formed complex phosphorylates SMAD1 and SMAD5. These actions inhibit SMAD2/3. A pro-fibrotic phenotype is promoted by the SMAD1/5/4 complex. The pathway regulation interacts with SMAD4 to associate with the SMAD1/5 complex131. By activating canonical WNT signaling, TGF β1-stimulated β-catenin accumulates in the nucleus, resulting in increased expression of T-cell factor/lymphoid enhancer binding factor-1(TCF/Lef-1) transcription factors, fibrotic lesion development, and increased numbers of myofibroblasts132.

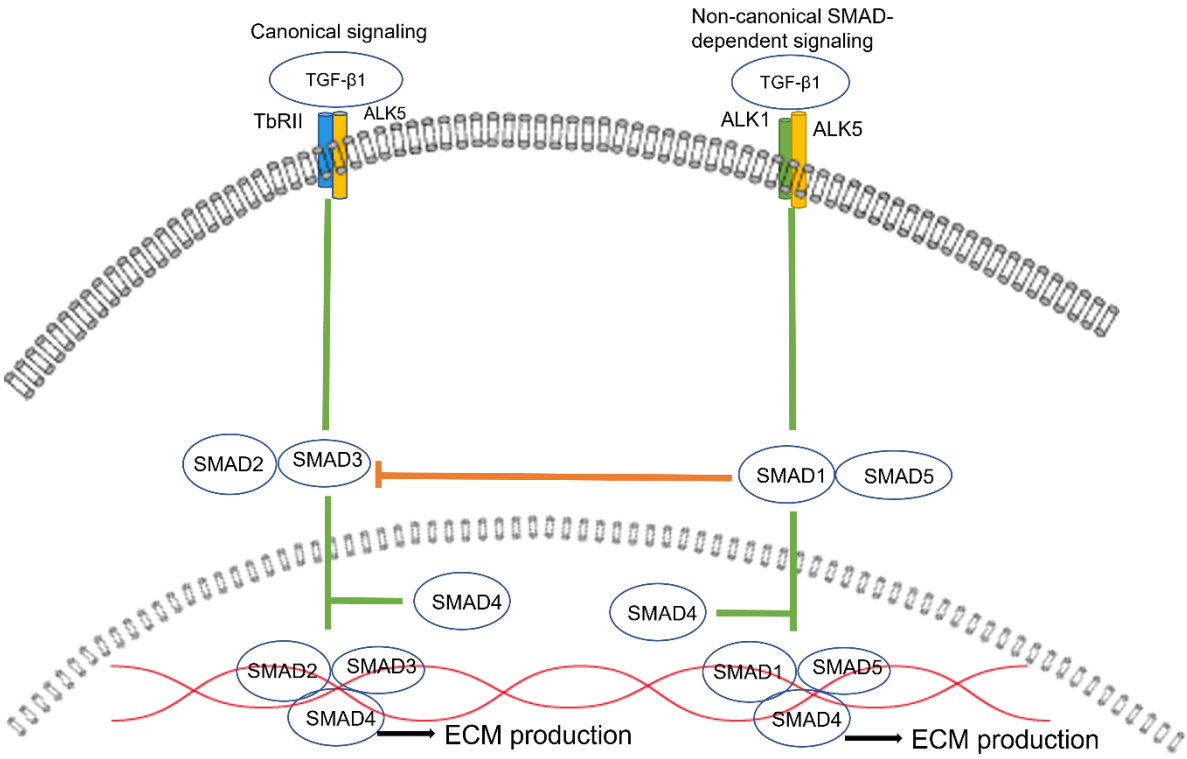

Figure 4. The activation of non-canonical and Smad-dependent transcriptional pathways in fibroblasts. Two types of TGF-β1 receptor (ALK5 or ALK1) are known to bind to TGF-β1 and type II receptors (TbRII). ALK5 is

responsible for activating Smad2/3, while ALK1 is responsible for activating Smad1. Even though TbRII-ALK5-Smad2/3 play a relatively well-established role in fibrosis, ALK1-Smad1/5's relevance to fibrosis remains unclear. The fibrotic response may also be mediated by TGF-β-mediated activation of non-Smad cascades (Figure was created with Adobe Illustrator 2021).

The role of WNT signaling in fibrotic disorders has been extensively studied and, more specifically, WNT/β-catenin signaling has been suggested to contribute to fibrotic mechanisms across different organs, tissues, and cells[133]. Frizzled (Fz) receptors are members of the transmembrane receptor family that bind soluble Wnt ligands[134]. When the Wnt turn off, glycogen synthase kinase 3β (GSK3β), and casein kinase 1 (CK1) are two components of the β-catenin proteasomal degradation that are phosphorylated by internal WNT inhibitors in excess of WNT ligands, leading to the destruction of cellular β-catenin. resulting in the destruction of cytoplasmic β-catenin[135, 136](Figure 5). β-catenin is subsequently phosphorylated, ubiquitinated, and proteasomally degraded during these events. When the Wnt turn on, an activation of the downstream signaling cascade by ligands is based on the engagement of the Fz receptors, together with the co-receptors Low-density lipoprotein receptor-related protein 5 (LRP5) and LRP6. A combination of GSK3 and CK1 phosphorylates LRP in its cytoplasm[137-139]. Disheveled (DVL), Axin, and GSK3β interact with the activated Fz/LRP complex[138, 139]. By directly interacting with the destruction complex, β-catenin, GSK3, CK1, adenomatous polyposis coli (APC), and the enzyme that binds to ubiquitin, Axin functions as a scaffold for the degradation process. Because the Fz/LRP complex sequesters Axin and GSK3β to the plasma membrane, the ubiquitin ligase is excluded from the degradation complex, preventing β-catenin ubiquitination and degradation[140]. In the nucleus, stabilized β-catenin interacts with TCF/Lef-1 transcription factors in order to regulate target gene expression[141, 142].

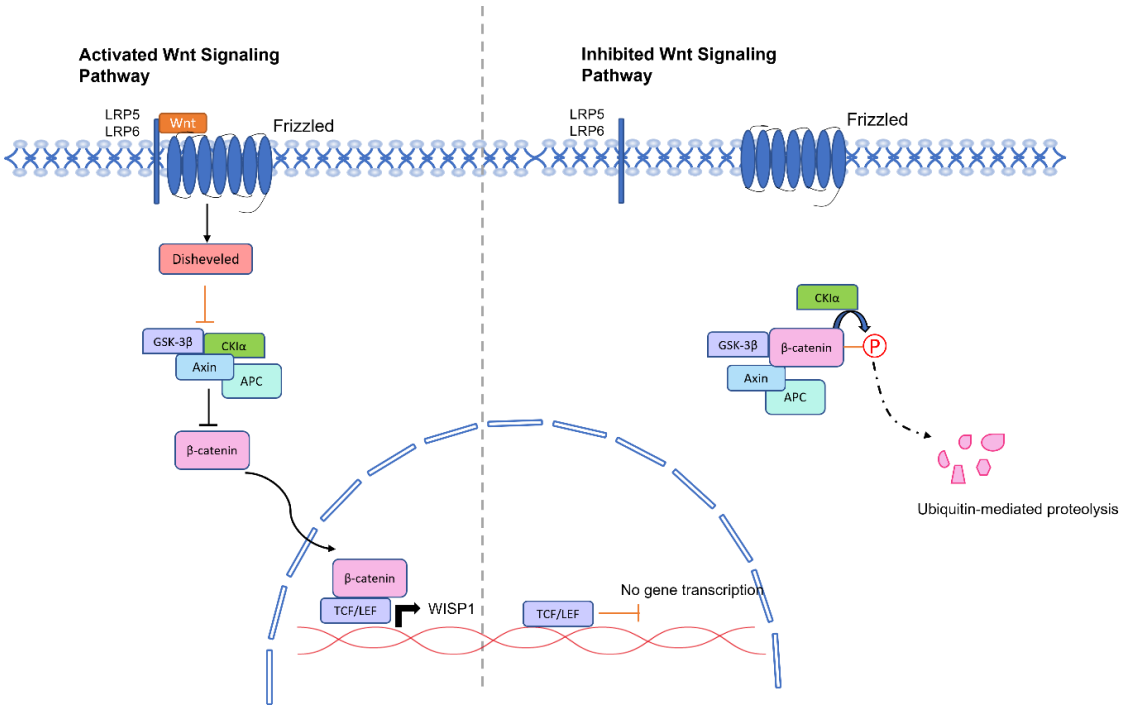

Figure 5. Canonical Wnt signaling in fibrosis. The canonical WNT cascade shown as an activated and non-activated chain with translocation of β-catenin (Figure was created with power point).

Multiple studies have demonstrated interactions between the Wnt and TGF-β1-SMAD signaling pathways during fibrosis [136, 143-145]. Previously, researchers demonstrated that crosstalk between TGF-β1 signals and β-catenin signaling played an important role in the progression of myocardial fibrosis and myofibroblast differentiation[146]. TGF-β1 can stimulate phosphoinositide 3-kinase /Akt (PI3K/Akt) pathway and collaborate with Wnt signaling[147](Figure 6). It was therefore shown that TGF-β1 activation of the Wnt pathway caused Wnt secretion through the Wnt pathway. Furthermore, TGF-β1-induced myofibroblast transformation could be blunted by inhibiting β-catenin[146]. It can be concluded that transformative and fibrogenic processes require crosstalk between Wnt and TGF-β1-SMAD signaling.

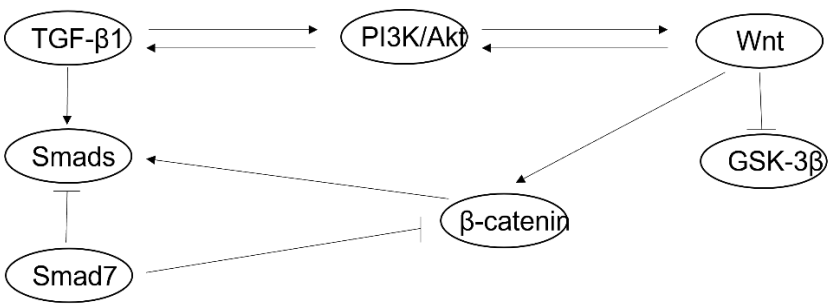

Figure 6. TGF-β signaling interacts with Wnt signaling pathway. (Figure was created with power point)

2. Material and Methods

2.1 Materials

2.1.1 List of the antibodies

Primary antibodies

Antibody	Dilution	Antibody Registry Number	Supplier
Anti-Ki67 antibody produced in rabbit	1:500	SAB4501880	Sigma-Aldrich Chemie GmbH
alpha smooth muscle actin (α - SMA)	1:100	M0851	Dako
Recombinant Human WISP-1/CCN4 protein	40ng/ml	1627-WS-050	R&D system
Recombinant Human TGF-beta 1 Protein	0.5ng/ml	240-B-002/CF	R&D system
Vimentin	1:250	Ab92547	Abcam
WISP1	1:500	Ab155654	Abcam

Secondary antibodies

Antibody	Catalogue number	Application	Source
Goat anti-rabbit IgG 594, Alexa Fluor	1851471	IF	Thermo Fisher Scientific
Goat anti-rabbit IgG 488, Alexa Fluor	1885240	IF	Thermo Fisher Scientific
Goat anti-mouse	1830459	IF	Thermo Fisher

IgG 594, Alexa Fluor			Scientific

2.1.2 Chemicals and Reagents

Chemical/Reagent	Product number	Source
2-Mercaptoethanol	60-24-2	Sigma Aldrich Merck
Acetic acid	818755	Merck Biosciences (Darmstadt, Germany)
ACK Lysing Buffer	A1049201	Thermo Fisher
Albumin Fraction V(BSA)	T844.3	Carl Roth GmbH
Bouin's solution	HT10132	Sigma Aldrich Merck
Citric acid	C1909	Sigma-Aldrich Chemie GmbH
Collagenase, type IV	17104019	Thermo Fisher
4,6-diamidino-2-phenylindole (DAPI)	Ab228549	Abcam
Dulbecco's Phosphate Buffered Saline	D8537	Sigma-Aldrich Chemie GmbH
Dimethylsulfoxid (DMSO)	472301	Sigma-Aldrich Chemie GmbH
Dispase II	17105041	Thermo Fisher
Ethanol 70%	7078027	Otto Fischer GmbH
Ethanol 96%	7138032	Otto Fischer GmbH
Ethanol absolute	7127114	Otto Fischer GmbH
Ethanol absolute	64-17-5	Merck KGaA
Fast Green FCF	F7252	Sigma-Aldrich Chemie GmbH
Fetal Bovine Serum (FBS)	0010	ScienCell
Fetal Bovine Serum (FBS)	F7524	Sigma-Aldrich Chemie GmbH
Fetal Bovine Serum (FGS)	2352	ScienCell

Fibroblast Medium (FM)	2301	ScienCell
Fluorescence Mounting Medium	S3023	Daki Deutschland GmbH
Formaldehyde	4979.1	Carl Roth GmbH
Hank's balanced salt solution (HBSS)	14175079	Thermo Fisher
HCl (Hydrochloric acid) 37%	4625.1	Carl Roth GmbH
KAPA SYBR FAST qPCR Master Mix for LightCycler 480	KK4611	Sigma Merck
MTT	M6555	Sigma Merck
Natriumchlorid (NaCl)	3957.2	Carl Roth GmbH
Normal goat serum	50062Z	Life technologies
Penicillin-Streptomycin	P0781	Sigma-Aldrich Chemie GmbH
Penicillin-Streptomycin	0503	ScienCell
Phallodin-Atto 594	51927	Sigma Aldrich Merck
Roticlear	A538.1	Carl Roth GmbH
Tris base	T1503	Sigma-Aldrich Chemie GmbH
Tris-HCl	T3253	Sigma-Aldrich Chemie GmbH
Triton X 100	3051.2	Carl Roth GmbH
Trizol	15596018	Thermo Fisher
Tween 20	9127.2	Carl Roth GmbH
Trypsin-EDTA (ethylenediaminetetraacetic acid) (0.25%)	25200056	Thermo Fisher

2.1.3 Buffer and Solutions

Immunohistochemistry and Immunofluorescence

10x Tris Buffered Saline (TBS)

Tris base	24.2g
NaCl	85g
Distilled Water	800mL
Adjust pH to 7.4 with	5M HCl
Constant volume with distilled water to	1000mL

10x Phosphate-buffered saline (PBS)

PBS	9.55g
Tween 20	1mL
Constant volume with distilled water to	1000mL

20x Citrate buffer

Cutric acid (Monohydrate)	21g
Distilled Water	300mL
Adjust pH to 7.4 with	5M NaOH
Constant volume with distilled water to	500mL

Washing Buffer (1x TBST)

10x TBS	100mL
Tween 20	1mL
Constant volume with distilled water to	1000mL

Washing Buffer (1x PBST)

10x PBS	100mL
Tween 20	1mL
Constant volume with distilled water to	1000mL

2.1.4 Kits

Kits	Supplier
RNeasy Plus Mini Kit	QIAGEN
RT2 First Strand Kit (50)	QIAGEN
RT2 Profiler PCR Arrays	QIAGEN
Trichrome Stain (Masson) Kit	Sigma-Aldrich

2.1.5 Laboratory consumables

24/12/6-well plates	FALCON, Corning
96/48/24/6-well plates	Greiner Bio-one
6/10cm dishes	FALCON, Corning
Cell Strainer	FALCON, Corning
Cover slips	MENZEL-GLÄSER
96-well PCR microplate, Lightcycler-type	STARLAB
Syringe	Injekt, B/Braun
Tips	Eppendorf; Hamburg, Germany Kisker Biotech; Steinfurt, Germany

2.1.6 Laboratory equipment

Product	Manufacturer
Balance/Scale	SCAL TEC SBC 52
Biometra Tone	Analytik Jena
Centrifuge	Eppendorf
Freezer -20℃	LIEBHERR, Switzerland
Freezer -80℃	Heraeus, Thermo Fisher Sciemtific
GloMAX-Muti Detection System	Promega
Sterigard hood	Thermo Fisher Scientific, USA
HERAcell 150	Thermo Fisher Scientific, USA

iCycler	Bio-Rad, Hercules, CA
Imaging software	Olympus analysis software and Zeiss AxioVison
LightCycler 480 II system	Roche, Penzberg, Germany
Magnetic mixer	IKA-COMBIMAG RET
Microscopes	Olympus IX50 inverse microscope and Zeiss Axioplan 2
Microtome	Leica JUNG RM2055
Mithras LB 940 Microplate reader	Berthold Technologies, Wildbad, Germany
NanoDrop 1000 Spectrophotometer	Thermo Fisher, Waltham, USA
PH-meter	BECKMAN (Washington, DC, USA)
Photometer	Thermo-Labsystem Opsys MR
Pipettes	Eppendorf
Power supple	Bio RAD MODLL 200/2.0
Refrigerator 4℃	LIEBHERR
Shaker	IKA-Shaker MTS 4
Stereomicroscope	Zeiss Stemi 2000
Voter Mixer 7-2020	neoLab
Water bath	Lauda ecoline RE 104, MEDAX

2.1.7 Primary fibroblasts

A collection of CD patient surgical specimens was used to isolate human primary intestinal fibroblasts (HPIFs). Intestinal sections were used from the same patients both fibrotic section (fibrotic group) and non-inflammatory, non-fibrotic section (non-fibrotic/control group). The fibroblasts were isolated from Crohn intestinal tissue as described below. In fibroblast medium, all the cells were cultured in FGS (fibroblast growth supplement), 2% FBS (fetal bovine serum), and cultured in a humidified atmosphere of 7% CO2 at 37℃. Primary cells were used at passage 3 to 4.

2.1.8 Human Tissue

Three patients with CD were studied for tissue samples that needed to undergo surgery due to stenosis formation. In accordance with the Ethics Committee's approval, the study protocol has been approved by the Technical University Munich Hospital (number 233/17S). Where necessary informed consent was obtained from each subject for the study protocol. Samples were snap-frozen or placed in 4% paraformaldehyde (PFA) immediately after resection. As described below, human intestinal fibroblasts were isolated from CD patient's tissue.

Clinical, endoscopic, and pathological criteria were used to diagnose CD patients. In total, resection samples from 3 CD were included 2 men and 1 woman. The mean age of these patients' at diagnosis was 31.67±9.98y. Most patients had ileal disease 2(66.7%) vs. ileo-colic in 1(33.3%). The Montreal criteria including age, location, behaviour, perianal involvement and comorbidities are summarized in Table 4.

Table 4 Characteristics of all CD Patients Included in Study

Characteristics	**Patients (n=3)**
Clinical characteristics	3
Sex	
Male	2(66.7%)
Female	1(33.3%)
Age of diagnosis	31.67±9.98
Medications	
Anti-TNFs	2(66.7%)
Other biologics	1(33.3%)
Immunomodulators	0
5-ASA	0
Montreal criteria	
Age of diagnosis	
A1: <17	0
A2:17-40	2(66.7%)
A3: > 40	1(33.3%)

Location	
L1: ileal	2(66.7%)
L2: colonic	0
L3: ileocolonic	1(33.3%)
Behaviour	
B1: inflammatory	0
B2: structuring	3(100%)
B3: penetrating	0
Perianal involvement	
Yes	0
No	3(100%)
Comorbidities	
Psychiatric	0
Cardiac	0
Respiratory	0
Renal	0
Endocrine (diabetes, thyroid)	0
Anemia	0

Statistical data are presented in the form of mean±SD or number (%).

2.2 Methods

2.2.1 Primary fibroblasts isolation

Fibroblasts were obtained from diagnosed patients undergoing surgical intestinal tissue for their disease. Pieces were repeated washing with PBS (contain 1000UI/ml Penicillin and 1000UI/ml Streptomycin), and the tissues were immersed in 75% alcohol for 30 seconds(s). Then continued to wash the tissue with PBS 7-10minutes. Take out the tissue quickly and put them in 35mm diameter petri dish. And cut into tissue pieces about 1mm^2 in size. The epithelium was removed by using Hank's Balanced Salt Solution (HBSS) without Ca2+ and Mg2+ and EDTA (5 mM for 15 minutes at 37°C). Rinse the tissue in 20ml of ice-PBS. In order to digest

the rest of the tissue, 20U dispase II and 4000U collagenase D were used for 30 minutes at 37°C. Shake each tube up and down 2-4 times to break up the tissue. Pellet the tissue at 200*g in a tabletop centrifuge (4℃) for 5 minutes and pour off the supernatant and discard. Each pellet was resuspended by adding 10ml ACK lysis buffer and centrifuged to preserve the bottom cells. Added an additional FM and incubated the tissue culture dishes at 37°C in an incubator with 7% CO_2. After 24 hours, gently washed off non-adherent cells with two changes of HBSS.

2.2.2 Wnt signaling Array

384-Well qPCR-based microarrays for the human Wnt signaling pathway as well as a related SYBR Green-based qPCR mix were purchased from SABiosciences. The primer for 84 Wnt pathway genes and 5 housekeeping genes were precoated on the PCR array (PAHS-043Z).

The RT2 First-Strand cDNA synthesis kit was used to make cDNA from 1 g of RNA (SA Biosciences). The iCycler (Bio-Rad, Hercules, CA) was used to complete 40 cycles of amplification, with each cycle consisting of a 15-second denaturation at 95.0°C followed by 1 minute of annealing at 60.0°C.

2.2.3 Immunofluorescence assay

On coverslips in 6-well plates, $4*10^5$ cells were planted in 2ml FM with 2% FBS. First, cells were washed three times with PBS, followed by fixation in 4% PFA for 5 minutes at room temperature. Then, cells were washed twice with PBS and permeabilized in 0.5% TRITON X-100/PBS for 15 minutes at room temperature. Next, blocking was performed using goat serum (10%) for 30 minutes at room temperature, incubated overnight with the primary antibody diluted in blocking solution at 4℃. There were three times of washing the cells (5 minutes) with PBS the following day. Indirect immunofluorescence was performed by incubation with Alexa Fluor-488/594 conjugated secondary antibodies. Nuclei were counterstained with DAPI (1:10,000 in PBS). Finally, using a fluorescence microscope with a particular filter for distinguishing unique fluorescence, slides were placed in Fluorescence Mounting Medium and looked at. Zeiss software was used to take the pictures.

2.2.4 Immunohistochemistry assay

Before use, 4% PFA was used to fix and embedded fresh tissue, and 2.5µm sections were cut. The tissue section was deparaffinized and rehydrated as usual, followed by retrieval of antigen using the epitope retrieval method based on heat. In a brief, an acid buffer containing citrate acid was added to the sections after they were preheated (to sub-boiling temperatures) and microwaved for 10 minutes at sub-boiling or boiling temperature. Endogenous peroxidase was inhibited by a 10-minute bath in a room-temperature methanol solution containing 3% hydrogen peroxide. In TBS, 10% goat serum was used to block nonspecific reactivity. Following that, primary antibodies were applied overnight to tissue sections at 4°C. Afterwards, second antibodies were applied along with horseradish peroxidase, followed by color detection with diaminobenzidine (Liquid DAB+ Substrate Chromogen System, Dako) and counterstaining with Mayer's hematoxylin. To finish the technique, the samples were dehydrated and mounted using Permount (Vector Laboratories). Permeabilized sections were treated with TBST in 10 minutes if needed. Throughout the experiment, TBST buffer was utilized as washing buffers.

2.2.5 Hematoxylin and eosin staining

The deparaffinization of embedded tissue sections in paraffin (2.5 µm thick) was performed three times for 10 minutes each, followed by two minutes per series of decreasing alcohol (100%, 100%, 100%, 96%, 70%, 50%). Hematoxylin-stained slides were cleaned for 20 minutes under running water after staining. Eosin was used to stain the slides. A series of escalating alcohol concentrations was used to dehydrate the slides (50%, 70%, 96%, 100%, 100%, 100%, 100%, 100%, 2 minutes each) and then Roticlear was applied three times for 10 minutes each. Afterwards, mounting medium was applied to the slides.

2.2.6 Sirius red staining

The Sirius red staining was performed to evaluate the collagen deposition in the CD fibrosis. Collagens I and III were dyed red, and the cytoplasm was dyed yellow.

Therefore, the sections were stored after one hour at room temperature. After that, they were incubated for one hour at 58℃ in pre-heated Bouin's Solution. Wash the parts in running tap water for 10 to 15 minutes to remove the yellow hue. Then they were dyed for 20 minutes at room temperature with 0.1% Fast green (Fast Green FCF, Sigma-Aldrich). Rinsed for one minute in 1% acetic acid then discarded solution and flushed with tap water 5 minutes later. 30 minutes were required to completely stain the sections with Sirius red 0.1%. After that, the slides were dehydrated by immersing them in 70% ethanol for 10 seconds, 100% ethanol for 1 minute, and then 100% Toluol for 3 minutes. Finally, cover the slides with mounting media. The slides were left to dry at room temperature overnight.

The pathologist used a previously described semi-quantitative scoring system to grade the fibrosis from 0 to 4 (Table 5).

Table 5 Histologic score for fibrotic CD

Score	Fibrosis
0	No fibrosis
1	Minimal fibrosis in submucosa or subserosa
2	Increased submucosal fibrosis, septa into muscularis propria
3	Septa through muscularis propria, increase in subserosal collagen
4	Significant transmural scar, marked subserosal collagen

2.2.7 Masson’s trichrome staining

Masson’s trichrome staining was carried out as directly by the manufacture using a Masson’s trichrome staining kit. Incubation of sections in preheated Bouin's solution at 56 °C for 15 minutes after being wetted in deionized water for 2 minutes. The segments were stained for 5 minutes with Hematoxylin concentration at work after being washed with water to remove the yellow hue. After that, staining was performed by incubating the sections in Biebrich scarlet-acid fuchsin solution for 5 minutes at room temperature using Masson's trichrome stain kit (Sigma-Aldrich HT15), which contains the red dye Masson's trichrome, 5 minutes in a

phosphotungstic/phosphomolybdic acid concentration, 10 minutes in aniline blue solution, and 2 minutes in 1% acetic. Using Roti-Histol, the slices were sterilized, and a Roti-HistoKit was used to mount them after being dehydrated in 80% ethanol, 100% ethanol I, and 100% ethanol II for 5 minutes each (Roth 6638). In a white region, nuclear was labeled black, cells were coloured red, and collagen was colored blue. Trichrome photos were converted to CMYK for fibrotic area quantification, and a cyan channel was used to quantify collagen with blue staining.

2.2.8 MTT assay

The 3-(4,5-dimethylthylthiazol-2-yl)-2,5diphenyltetrazolium bromide (MTT) technique was used to assess the vitality of fibroblasts. MTT Assays were carried out with staggered concentrations of the several compounds that had been previously solubilized in DMSO. Cells were seeded in wells of 96-well plates ($2x10^3$ cells per well). After indicated treatments, 20 µL of MTT (5mg/ml) was added to each well. After 4 h at 37 °C in the dark, the MTT medium was removed and 150 µL of dimethyl sulfoxide (DMSO) was added to each well. The absorbance was measured at an optical density of 570 nm (OD570). Triplicates were carried out.

2.2.9 Scratch wound healing assay

For analysis of cell migration, scratch wound assays were performed. In detail, HPIFs were plated on a 6-well plate and following 24 hours of starvation in no FBS medium. To obtain a standardized scratch through the otherwise confluent cell layer, the cell layer was scratched once from edge to edge of the culture dish using a 20 µl micropipette tip. The cells were then rinsed in PBS and grown for 24 hours in fresh complete medium. The cells were then incubated in starvation no FBS medium which no reagents or TGF-β had been added. Photos of the scratches were taken at 0, 6, 12 and 24 hours after scratching with an Olympus IX50 inverted laser scan microscope using a 10 x 0.25 Ph1Var1 objective at room temperature. The migration rates were computed [(scratch area at 0 hour—scratch area at 24 hours)/scratch area at 0-hour *100 percent]. At least three distinct studies were used to get mean data, which were then normalized to the matching controls. Photographs were taken of the wounds observed under the microscope at different

time points, i.e., 0 h, 6 h, and 24 h.

2.2.10 RNA isolation from tissue and cells

A Trizol extraction method and a RNeasy Mini Kit were used to collect RNA from tissue and cells.

In order to prepare tissue, 30 mg of fresh tissue was placed in 400 µl of RLT along with 0.4µl of β-ME. The lysate was homogenized for five minutes, then centrifuged for three minutes in high centrifugal speed. The supernatant (350 µl) was taken away. Pipetting was used to mix 350 µl of 70% ethanol into the lysate. 700 µl of the sample was transferred to a RNeasy Mini spin column and spun for 15 seconds at 8000 g in a 2 ml collecting tube. The flow-through was thrown out. The RNeasy Mini spin column was filled with 700 µl of Buffer RW1. The flow-through was discarded after 8000 g of centrifugation was used for 15 seconds. We centrifuged buffer RPE (500 µl) for 2 minutes at 8000 g using the RNeasy spin column. The flow-through was thrown out. The RNeasy spin column was filled with buffer RPE (500 µl) and centrifuged for 2 minutes at 8000 g. To further dry the membrane, The RNeasy spin columns were centrifuged for 1 minute in new 2 ml collection tubes. New 1.5 ml collection tubes were used to house the RNeasy spin columns. Eluted RNA was extracted from spin columns by directly adding RNase-free water to the membrane and centrifuged for 1 minute at 8000g.

The cells were seeded either stimulated or unstimulated in 6-well plates. A kit for RNA isolation was used to extract total RNA from cultivated cells, as directed by the manufacturer. The culture media was removed, and the cells were quickly rinsed in PBS. Using a cell scraper, cells were scraped off of plates after adding 1ml Trizol, and collected into 1.5ml tubes. And then add 200µl Chloroform to each tube, vortex 1-2 minutes. The lysate was then centrifuge for 15 minutes at 12000rpm at 4℃. Afterwards, collected the upper layer liquid and transferred to a new tube. each tube was filled with 500µl isopropanol and incubated for 10 minutes. The mixture was then placed to a perfect RNeasy spin column and 10000 x g centrifuged for 15 seconds, with the fluid passing through being removed. RNA was preserved in perfect bind-RNA columns that were washed with wash buffers RW1 and RPE to remove cellular debris and other contaminants, ensuring that the columns contained only RNA. After centrifugation at 1000 x g for 2 minutes, the RNA-

containing columns were completely dried. After that, the column was placed in a new 1.5 ml tube and 30µl RNase-free water was added directly to the spin column membrane, which was then incubated for 3 minutes. After centrifuging the tubes for 1 minute at 10,000 x g to elute RNA. Take 1ul RNA sample and measure the OD value in the nano drop. If the ratio of OD 260/280 is greater than 1.8. It shows that the prepared RNA is relatively pure and free of protein contamination. Aliquots of RNA samples were kept at -80℃.

2.2.11 cDNA synthesis

Utilizing a cDNA synthesis kit, the cDNA transcription was performed as instructed by the manufacturer. Equal amounts of RNA (500ng-1g) and RNase-free water (varying volume, determined by RNA concentration) were added to an RNase-free tube. A total of 10 µl of RNA template and RNase-free water were used. 2 µl of Buffer GE was then added to the reaction tube (Table 6). The following protocol was used to reverse-transcribe RNA samples in a thermocycler: Place the genomic DNA elimination mix on ice for at least one minute after incubation for 5 minutes at 42°C. The reverse-transcription mix should be prepared according to Table 7. To each tube containing 10 l of the genomic DNA removal solution, add 10 l of the reverse transcription mixture. Pipette lightly up and down to combine. Incubate for exactly 15 minutes at 42 °C. After five minutes of incubation at 95 °C, immediately stop the process. Each reaction requires 180 µl of RNase-free water. Pipette many times up and down to combine. The reverse-transcription reactions were held at -20°C or put on ice and utilized for real-time PCR.

Table 6 Genomic DNA elimination mix

Component	Amount
RNA	25ng-5ug
Buffer GE	2µl
RNase-free water	Variable
Total volume	10µl

Table 7 Reverse-transcription mix

Component	Volume for 1 reaction	Volume for 2 reactions	Volume for 4 reactions
5x Buffer BC3	4 µl	8 µl	16 µl
Control P2	1 µl	2 µl	4 µl
RE3 Reverse Transcriptase Mix	2 µl	4 µl	8 µl
RNase-free water	3 µl	6 µl	12 µl
Total volume	10 µl	20 µl	40 µl

2.2.12 Quantitative reverse-transcription PCR (qRT-PCR)

Primer-BLAST (http://www.ncbi.nlm.nih.gov/tools/primer-blast/) and Primer Bank (https://pga.mgh.harvard.edu/primerbank/) were used to create primers. qRT-PCR was done with a KAPA SYBR FAST Kit in a Roche LightCycler 480 real-time PCR equipment. The relative mRNA expression levels were calculated by comparing them to HPPIB.

qRT-PCR primer sequences

Primer	Sequence Forward primer	Sequence Reverse primer
hPPIB	TGTGGTGTTTGGCAAAGTTC	TGTGGTGTTTGGCAAAGTTC
Col1A1	CCTGGAAAGAATGGAGATGATG	ATCCAAACCACTGAAACCTCTG
Col3A1	GCTGGCTACTTCTCGCTCTG	TCCGCATAGGACTGACCAAG
Fibronectin	CCACCCCCATAAGGCATAGG	GTAGGGGTCAAAGCACGAGTCATC
Vimentin	GACCAGCTAACCAACGACAAA	GAAGCATCTCCTCCTGCAAT
TIMP-1	ATACTTCCACAGGTCCCACAAC	GGATGGATAAACAGGGAAACAC
MMP2	GATACCCCTTTGACGGTAAGGA	CCTTCTCCCAAGGTCCATAGC
SFRP4	GGACCCTGCCAAGTTCAAGA	ACGGCATACGTGTCGTAGTC
IL-6	TACCCCCAGGAGAAGATTCC	TTTTCTGCCAGTGCCTCTTT

WISP-1	GTATGTGAGGACGACGCCAAG	GGCTATGCAGTTCCTGTGCC

qRT-PCR reaction component

Target Gene	hPPIB
0.4 µl RT-forward primer	0.4 µl hPPIB-forward primer
0.4 µl RT-reverse primer	0.4 µl hPPIB-reverse primer
5.2µl H_2O	5.2µl H_2O
Total volume 20µl	5.2µl H_2O

qRT-PCR cycling protocol

Temperature	Time
1. 95 ℃	5 minutes
2. 95 ℃	10 seconds
3. 60 ℃	10 seconds
4. 72 ℃	10 seconds
5. 45 cycles for step 2-4	
6. Melt-curve analysis: hold times of 5 seconds at 95°C, 1 minute at 65°C, and 97°C will be repeated	
7. 40 ℃	30 econds

2.2 Statistics

Data collected from this study are expressed as the mean ± SEM and were statistically analyzed using Student's t-test or one-way analysis of variance (ANOVA), followed by Tukey-Kramer test. A statistically significant value was defined as $p<0.05$. The correlation of WISP-1 and fibrosis score was assessed using Spearman's method as described[148].

3. Results

3.1 WISP-1 expression is upregulated in fibrotic regions in CD

3.1.1 The changes in the histomorphology of CD fibrosis

Fibrosis combined with smooth muscle layer increase, lessen and stiffen the bowel segment and result in strictures. Strictures in CD can occur anywhere in the digestive tract with the terminal ileum being affected in most cases. When compared to its macroscopically normal adjacent terminal ileal counterpart, the diseased section displays penetrating thickening of layers, stenosis and even obstruction (Figure 7A+B).

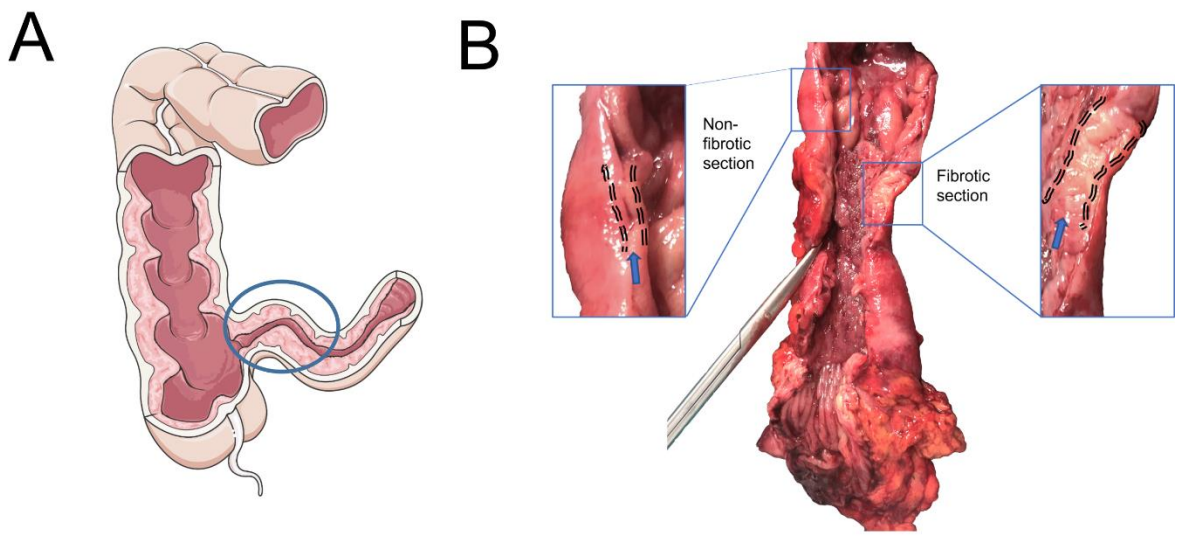

Figure 7. Morphological changes of fibrosis in CD. (A) A schematic of fibrosis and stricture of CD. (B) Segmental involvement with transmural inflammation and a stricture. The left blue arrow displays normal adjacent sections (non-fibrotic), while the right blue one shows a stricture site (fibrotic) from a patient with CD.

3.1.2 Analysis of WISP-1 from CD fibrosis tissue specimens

Since Wnt signaling components have been described to be involved in intestinal inflammation, we were interested whether changes could also be detected in samples from patients with intestinal fibrosis in CD. With the use of a Wnt signaling-specific PCR array, expression of 84 Wnt-mediated signal transduction genes was analysed in fibrotic regions and respective non-fibrotic/non-inflamed regions of the same patients. Our RNA-seq raw counts were visualized as a heatmap with hierarchical clustering and as a principal component analysis (PCA) representing the principal components of the data. As depicted in Figure 8A+B, several Wnt signaling components were differentially expressed in the fibrotic tissue compared to control.

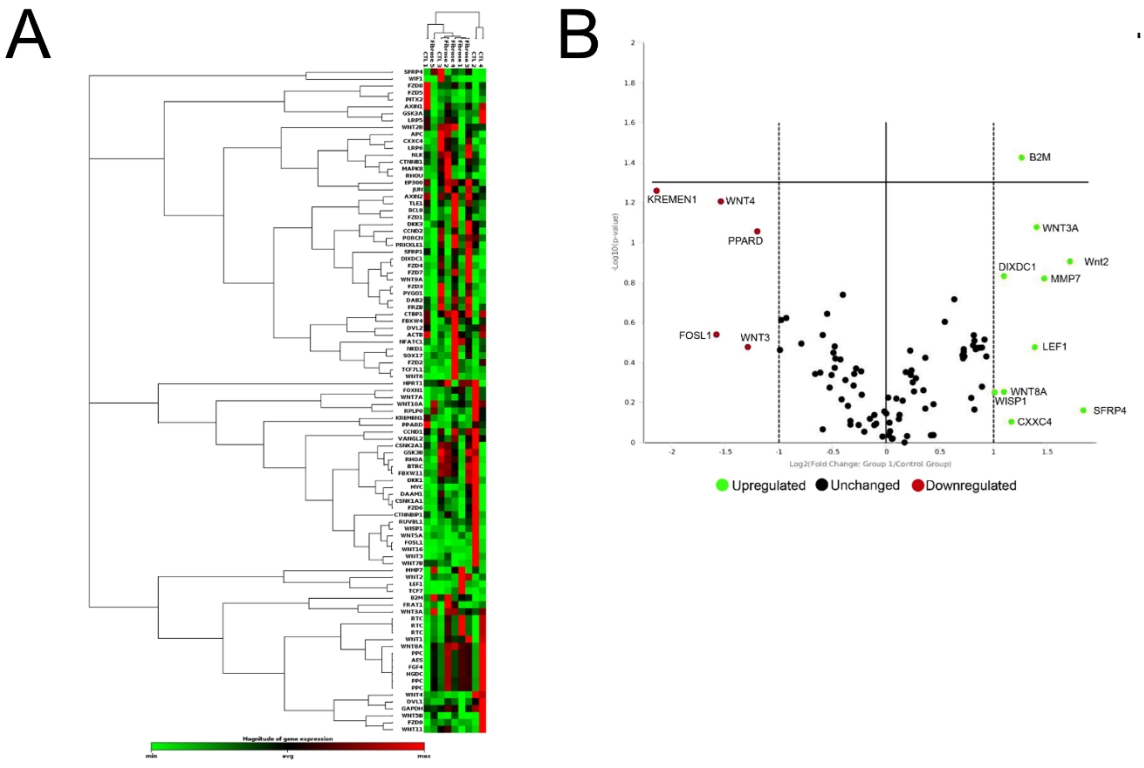

Figure 8. WISP-1 gene of non-fibrotic and fibrotic sections are distinct in the same patient's tissue RNA-seq. (A) Hierarchical clustering and gene expression heatmap across the 84 most classic expressed Wnt related genes in 5 fibrotic groups and 4 control groups were performed. Values are plotted relative to the average of non-fibrotic(control) group; (B) Volcano plot of Wnt signaling PCR array. PCR array analysis of gene expression in fibrotic sample in comparison to control group (n=6). The relative expression levels for each gene depicted as

log2(Group 1/Control Group) are plotted against -Log10(p-value). Red indicator= significantly down-regulated gene; Green indicator= significantly up- regulated gene.

As shown in Figure 9, qRT-PCR was used to analyse the mRNA from different sections of the CD's body to determine the expression of WISP-1. Expression of WISP-1 mRNA was significantly increased in the fibrotic tissue compared to pared non-fibrotic tissue (Figure 9).

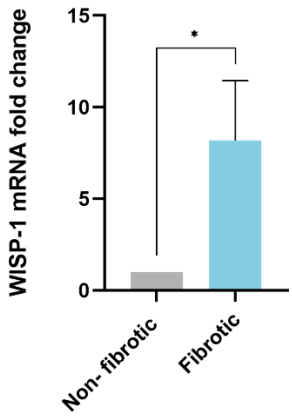

Figure 9. qRT-PCR of WISP-1 in resected specimen from patients with CD. Expression levels are normalized to non-fibrotic region samples. n=20. *p < 0.05.

3.2 WISP-1 expression can be located in the inflammatory transition zone between inflammation and fibrosis

3.2.1 Histological changes in CD fibrosis

Histomorphologic analysis of different sections of stenosing CD was performed. Massive hypertrophy (extreme volume increase) of muscularis propria smooth muscle, hyperplasia of smooth muscle, and replacement of typical loose connective tissue in H&E staining. Compared with the control group, fibrosis is markedly associated with increased collagen deposition, visualized by H&E staining (Figure10).

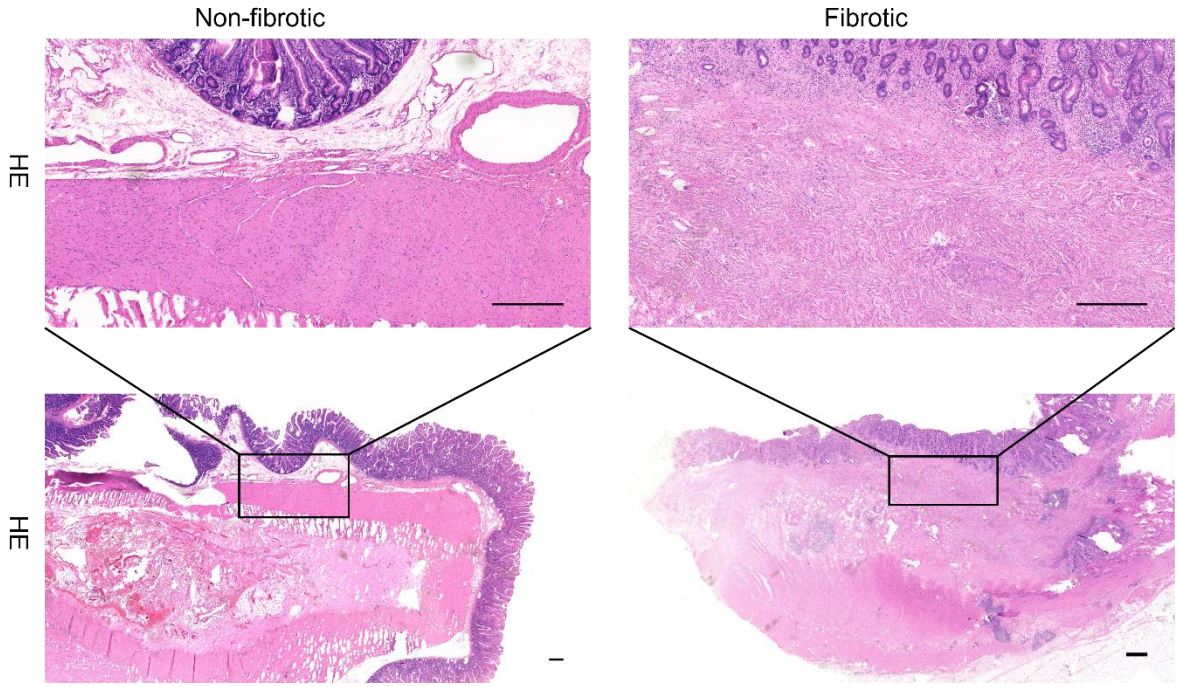

Figure 10. Representative H&E staining images of major histological features in a patient with fibrotic CD. The staining was conducted on human tissue slices of patients with stenosing (right panel) and non-fibrotic (left panel) intestinal sections. The scale bar: 500µm.

To demonstrate the presence of collagen fibers, sections were stained with Sirius red staining. In spite of Sirius Red's sensitivity to collagen, it cannot differentiate different subclasses of collagen. Sirius Red staining showed evidently apparent collagen fibers (red color) in the fibrotic sections rather than in the non-fibrotic intestine (Figure11).

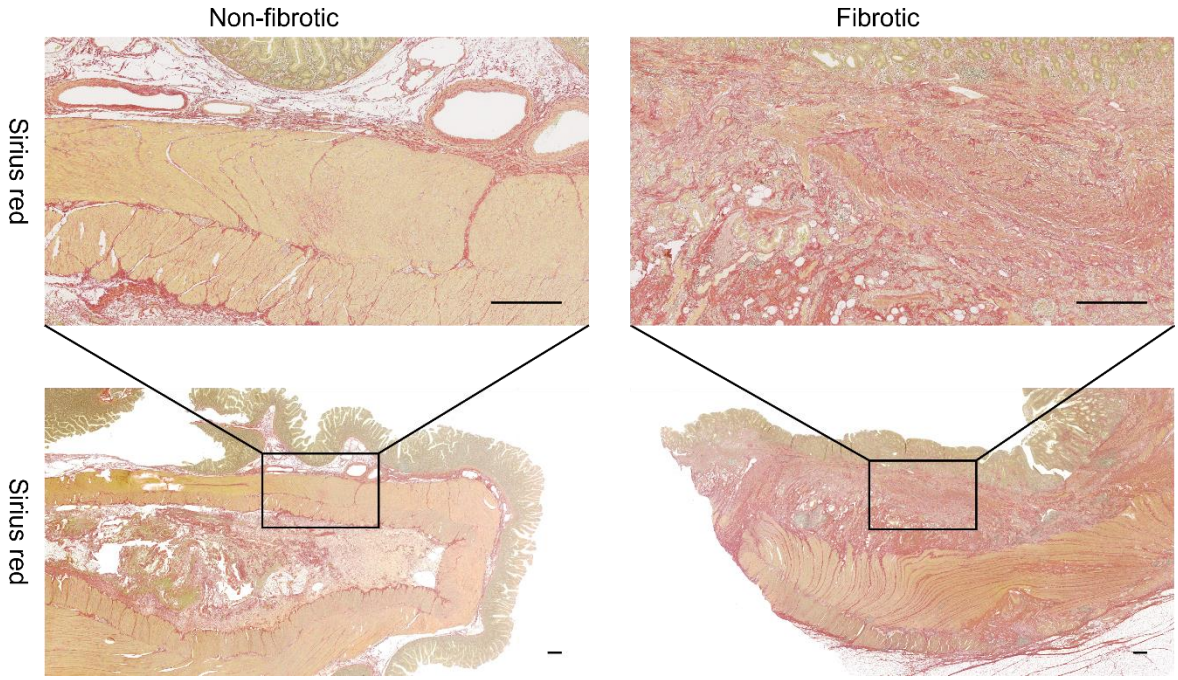

Figure 11. Representative micrographs of Sirius red staining of different CD fibrosis sections. The scale bar: 500μm.

We also used Masson trichrome staining to detect the extent of fibrosis of CD aside from and with stenosis. For the non-fibrotic tissue, submucosa, and lamina propria are a few blue, but there is no staining in the subserosa. An abundance of rich blue collagen fibres in the submucosal and subserosal tissues of CD patients can be seen in the regions with stenosis (Figure 12). This is how the fibrosis component appears on Masson's trichrome stain (in blue). Its location and extent are identical to those seen on Sirius red and H&E staining.

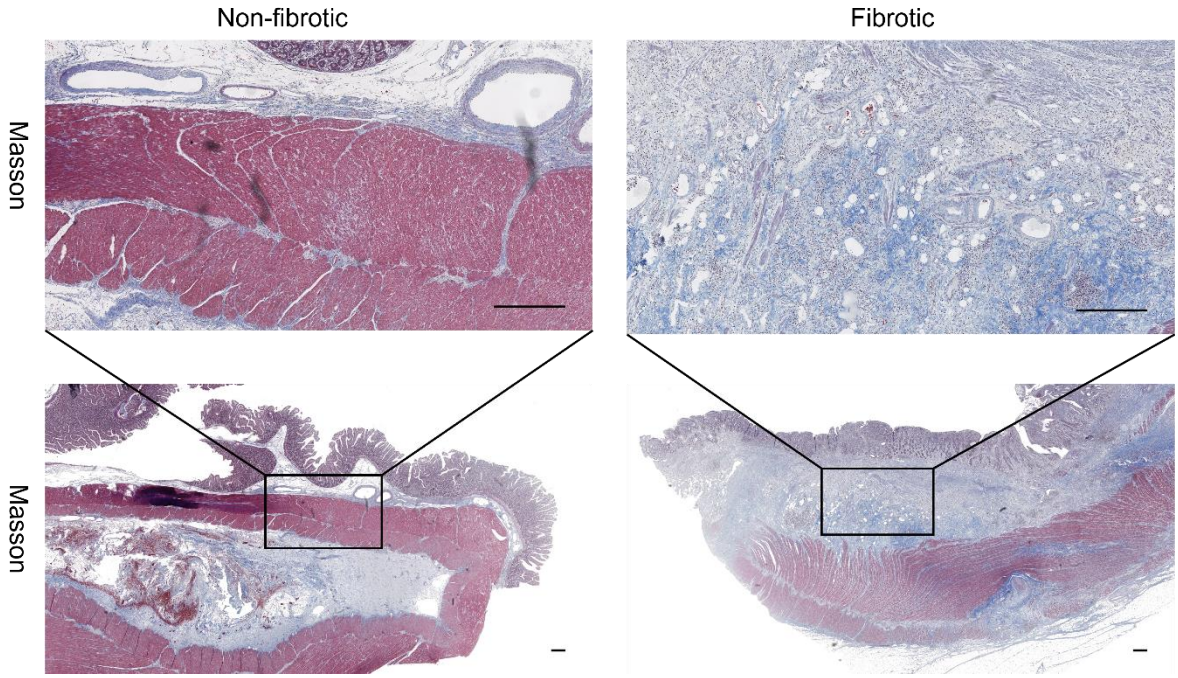

Figure 12. Representative images of Masson trichrome stained human intestinal tissue samples from CD patients in a non-fibrotic and fibrotic region. The scale bar: 500µm.

3.2.2 WISP-1 expression is upregulated in fibrotic regions in CD

To identify regional expression patterns of WISP-1 within the intestinal wall and compare WISP-1 expression in fibrotic and non-fibrotic regions, immunohistochemistry was performed using primary anti-WISP-1 antibodies (Figure 13A). WISP-1 expression was upregulated in fibrotic regions. Additionally, significantly higher WISP-1 expression was found in pre-fibrotic inflammatory regions compared to control (Figure 13B).

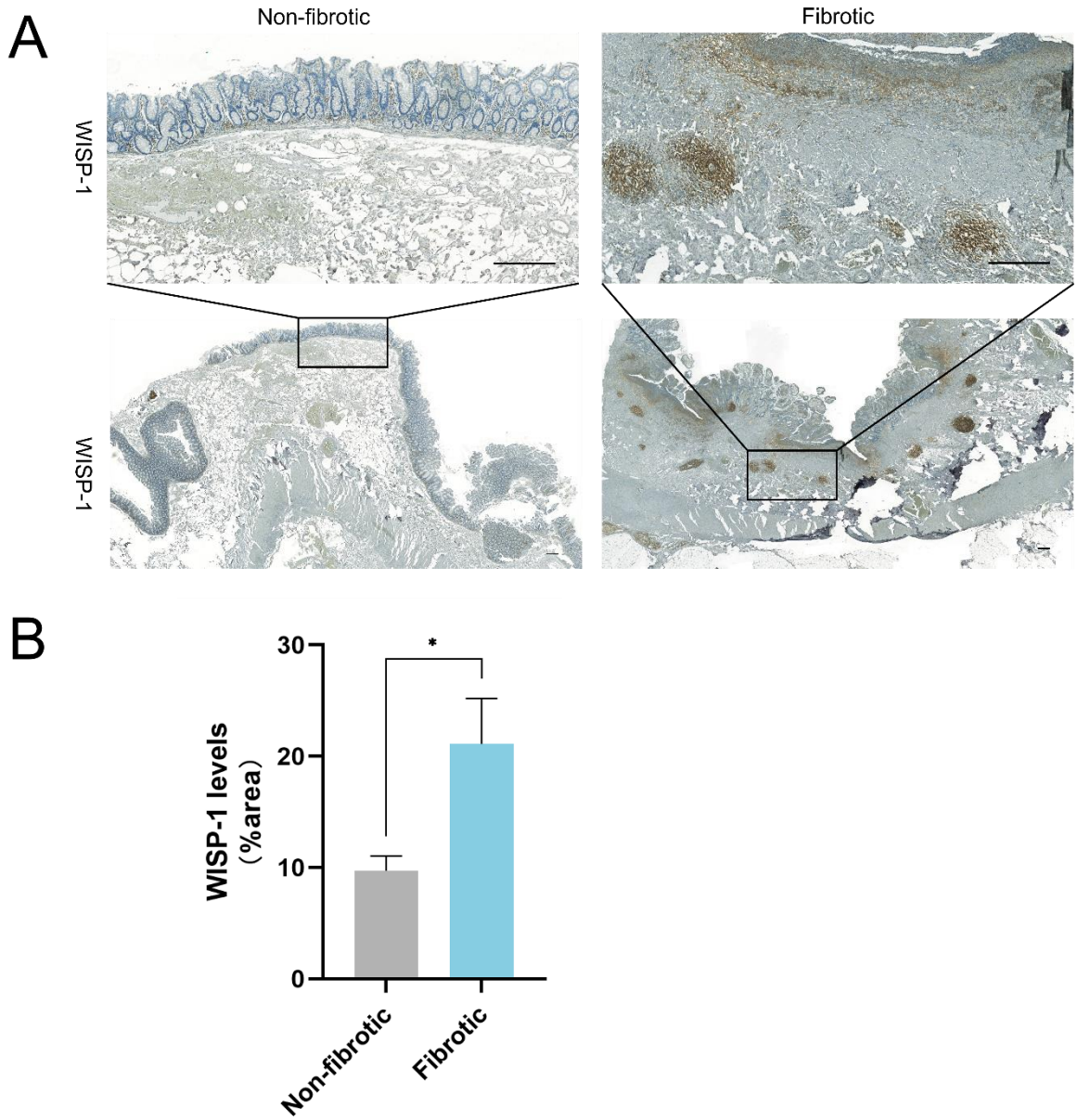

Figure 13. WISP-1 expression was increased in intestinal fibrosis in CD. (A) Representative immunohistochemistry sections of WISP-1 staining in CD intestinal samples. The scale bar: 500μm. (B) Quantification of WISP-1 expression area in CD samples using Image-Pro plus. n=3. *p < 0.05.

3.2.3 WISP-1 levels correlate with the intestinal fibrosis degree in CD fibrotic tissue

To explore whether the WISP-1 levels are associated with the fibrosis severity, 20 CD samples with histologic score were analyzed. As shown in Figure 14, WISP-1 mRNA expression in qPCR and fibrosis score showed a positive correlation in fibrosis tissue using the spearman's correlation. (r_s=0.8137, p<0.0001).

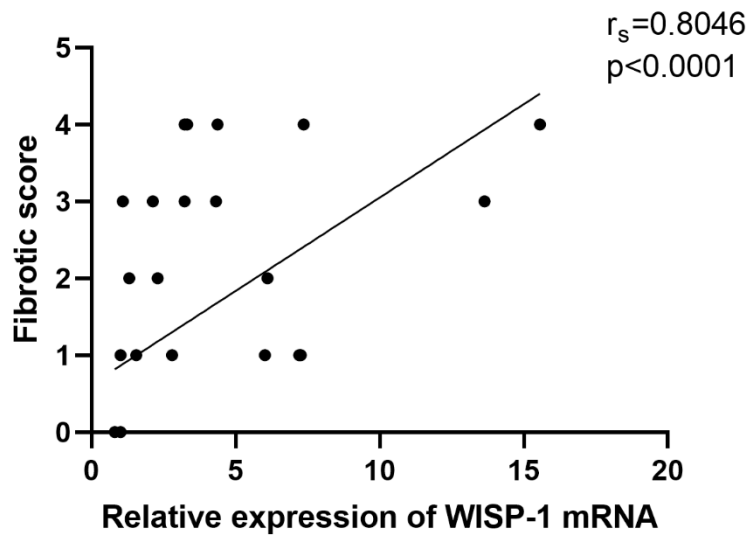

Figure 14. The WISP-1 levels correlate with intestinal fibrosis score in CD patients. The WISP-1 mRNA expression levels were positively correlate with the fibrotic score in the CD fibrosis patients (r_s=0.8137, p<0.0001).

3.3 Characterization and ECM production changes of fibrosis associated intestinal fibroblasts

3.3.1 Intestinal fibroblast cells

Since fibroblasts play a significant role in fibrosis formation, by secreting extracellular matrix components [149], we isolated them from fibrotic as well as control tissue of the same patients. For characterization of activated fibroblast, the markers α-SMA and vimentin were used (Figure 15). In addition to each immunostaining, a negative control with different cell line was performed (Figure 16). As shown in figure 15, isolated primary intestinal fibroblasts are all activated myofibroblasts.

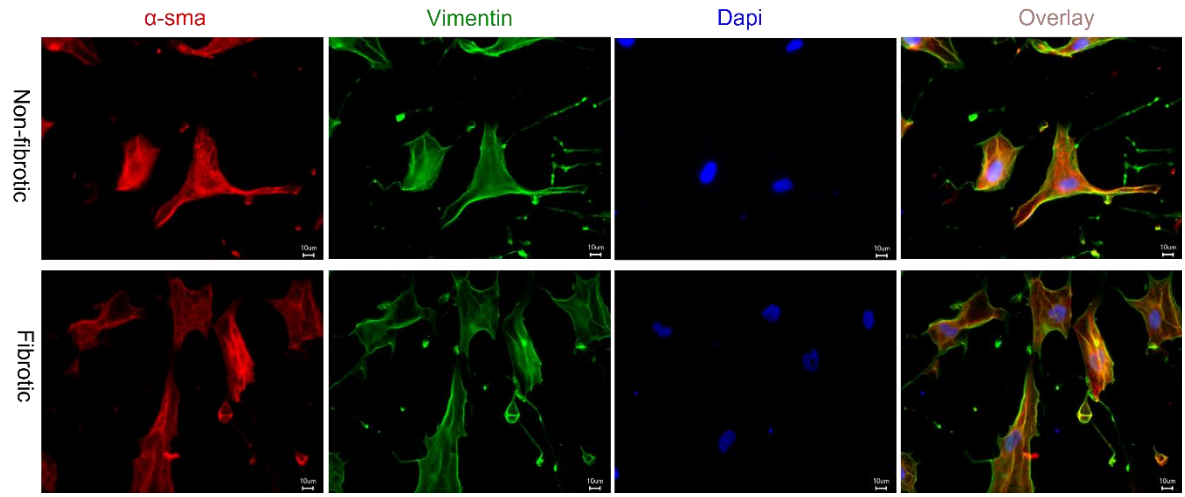

Figure 15. Characterization of primary fibroblasts from human intestinal tissue. (A) Immunofluorescence staining of α-SMA (red) vimentin (green) and DAPI (blue) shows that isolated intestinal fibroblasts are activated towards myofibroblasts. Scale bar: 100µm.

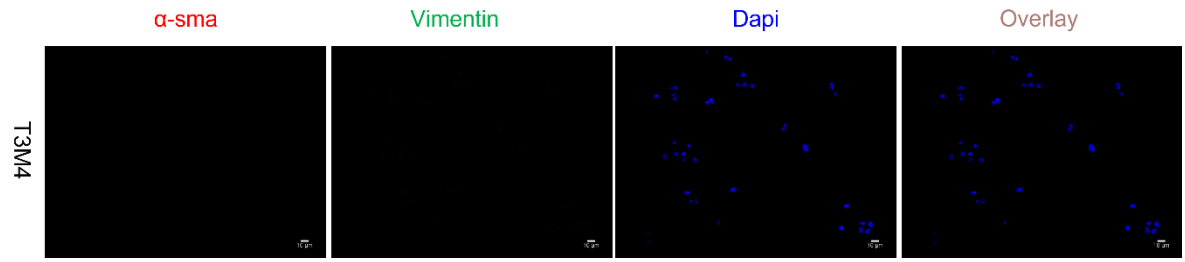

Figure 16. Representative immunofluorescence staining pattern of T3M4 pancreatic cell line. Cells were used as a negative control. DNA was stained positive with DAPI (blue) but α-SMA (red) and vimentin (green) were negative. Scale bars: 10µm.

3.3.2 ECM homeostasis is mediated by fibroblasts

To evaluate the extent of ECM production in non-fibrotic and fibrotic fibroblasts, qRT-PCR analysis was performed. This experiment showed that Col1A1, Vimentin, Fibronectin, and TIMP1 mRNA expression levels were higher in the fibrotic group compared to control group, but we could not detect any changes in Col3A1 between the two groups. In contrast to above genes, MMP2 mRNA expression level was lower in fibrotic compared to the non-fibrotic group (Figure 17). These results suggest that different fibroblasts respond differently in terms of ECM synthesis and degradation.

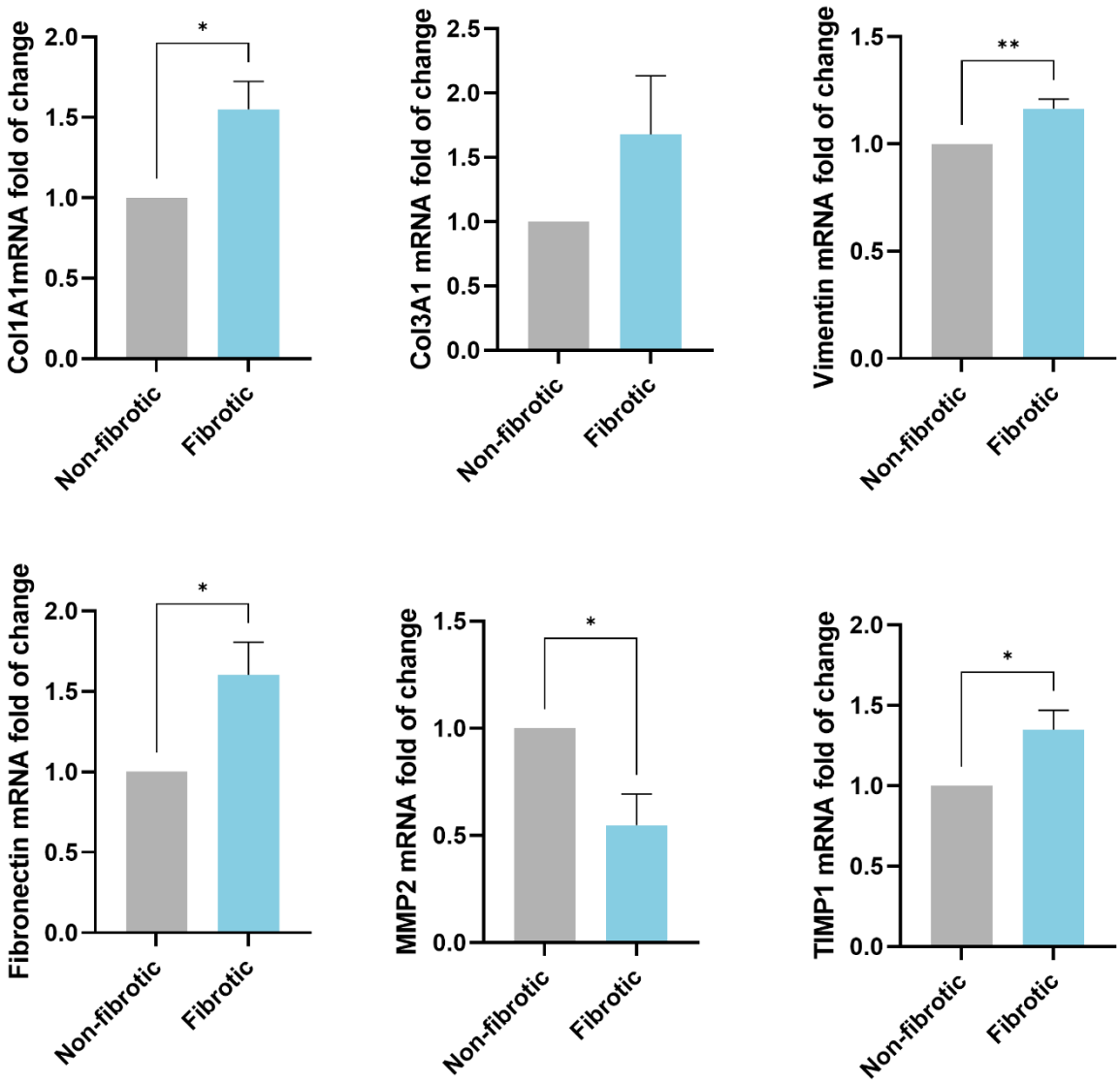

Figure 17. Effects of HPIFs on relative mRNA expression of ECM components. Bars represent the mean ± SEM (*p < 0.05; **p < 0.01; *** p< 0.001; **** p< 0.0001; n=3).

3.4 Fibroblasts behaviour changes during wound healing

3.4.1 Analysis of cell proliferation

Next, we investigated differences in functional aspects such as migration and proliferation. As a proliferation marker, the human Ki-67 antigen, is widely expressed in the nucleus during cell cycle progression150. As compared with the non-fibrotic group, HPIFs of the fibrotic group showed increased proliferation, as indicated by Ki-67- positive cells after 24h (Figure 18).

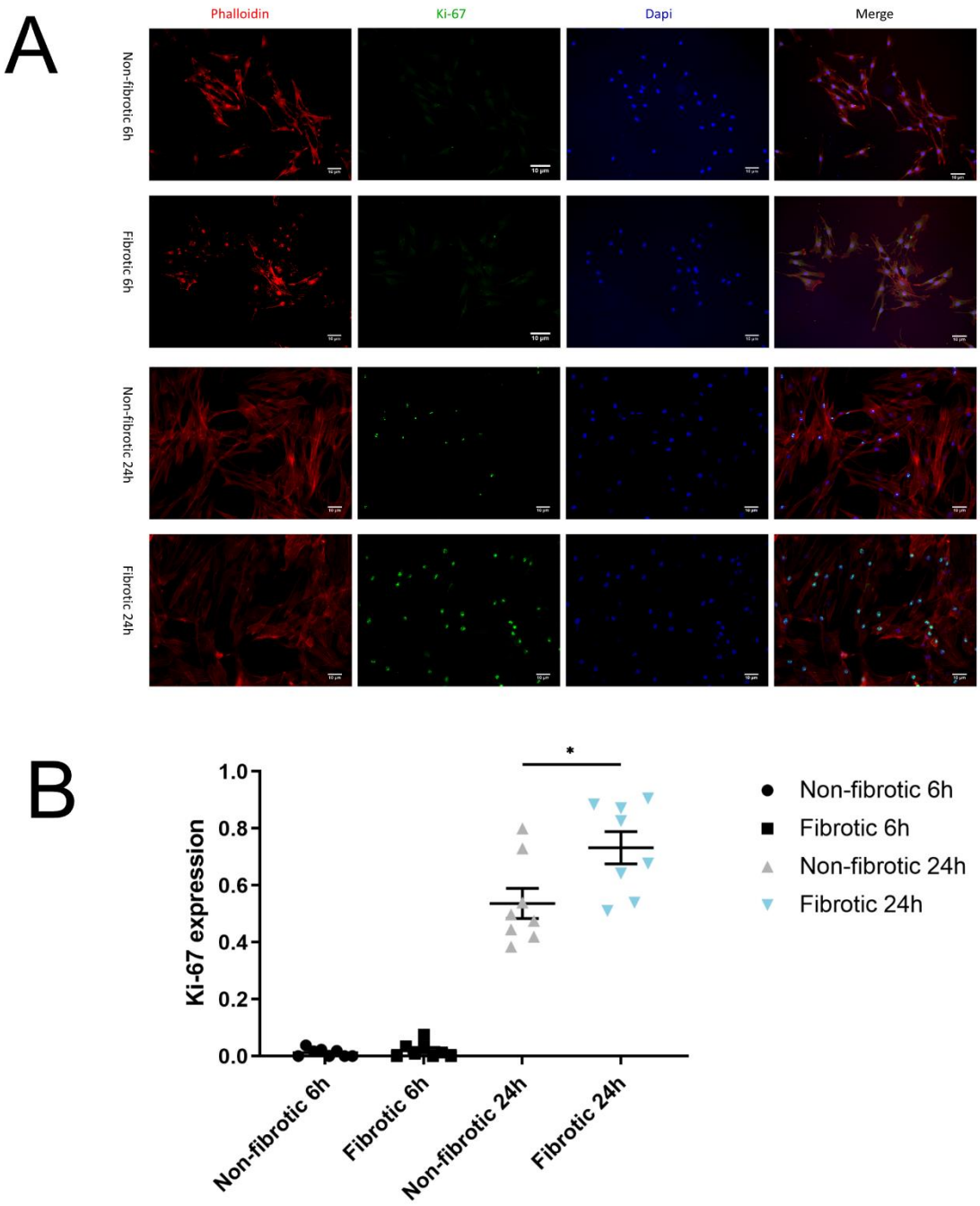

Figure 18. Ki-67 assay was used to measure cell proliferation. (A)The immunofluorescence staining and percentage of proliferating (Ki-67 positive) fibroblasts in the non-fibrotic and fibrotic group for 6h and 24h. Scale Bar: 10μm, *p < 0.05 compared with non-fibrotic group. (B) Cells positive for Ki-67 quantification. *p < 0.05 compared with non-fibrotic group.

3.4.2 Analysis of cell migration

To further characterize the cells with regard to their migratory activity, scratch wound assays were performed on different time points. Fibroblasts from the fibrotic regions showed significantly increased migratory activity resulting in enhanced wound closing compared to control fibroblasts from the non-fibrotic region (Figure 19).

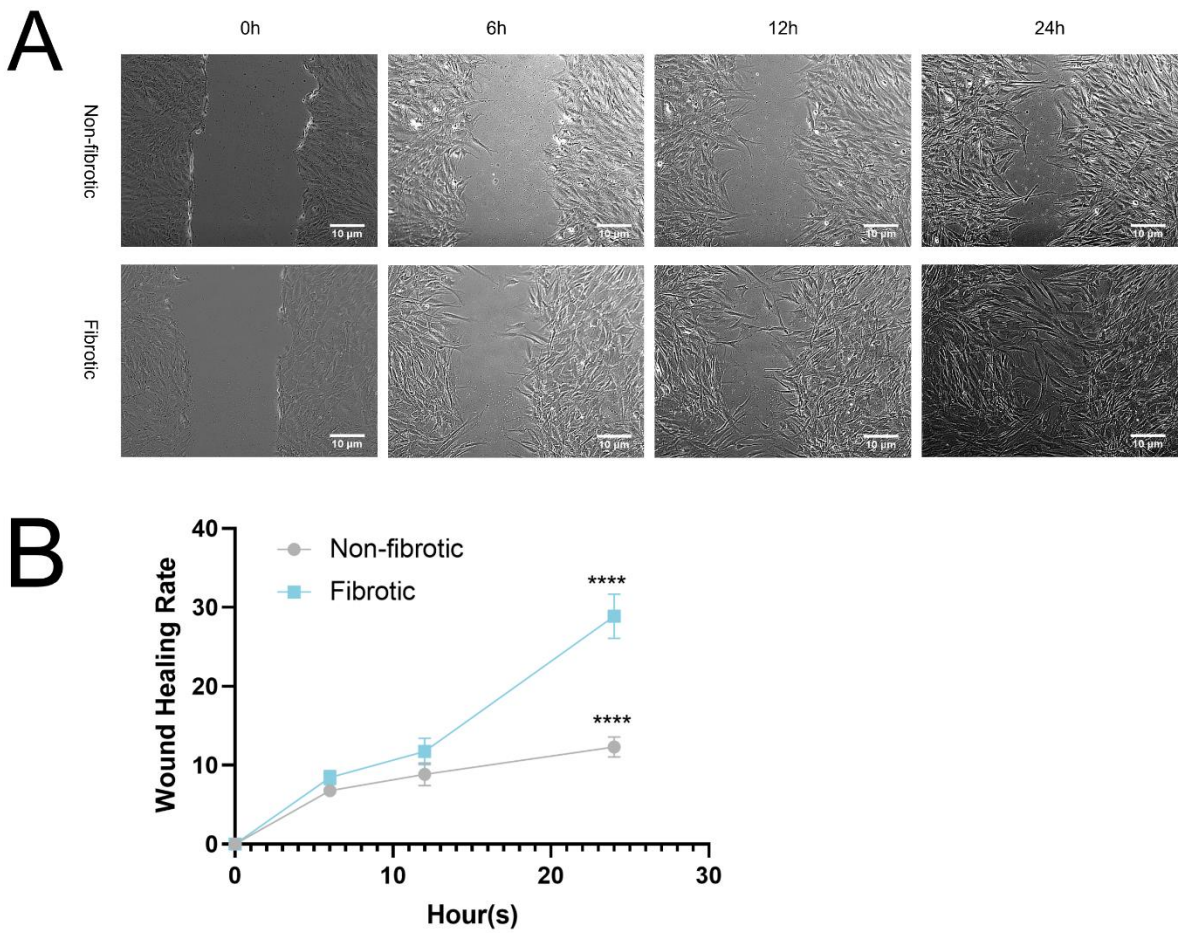

Figure 19. A comparison of the migration behavior of different groups of fibroblasts. (A) Representative images from in vitro scratch wound healing assays were recorded 0h, 6h, 12h, and 24h after wounding (scale bar: 50 µm). (B) Cell index curves showed wound healing (migration) rates over time (0h, 6h, 12h, 24h) for different groups of fibroblasts in the scratch wound test (*p < 0.05; **p < 0.01; *** p< 0.001; **** p< 0.0001; n=3).

3.5 Stimulation of primary human fibroblasts with TGF-β1 enhances WISP-1 expression

TGF-β1 is a critical cytokine implicated in the pathophysiology of fibrosis formation in numerous organs including the gut [151]. To mimic these profibrotic conditions *in vitro,* we investigated the effect of stimulating the primary human fibroblasts with TGF-β1. The optimal concentration of TGF-β1 is 0.5ng/ml (Figure 20). Stimulation of HPIFs with TGF-β1 led to increased expression of IL-6, especially in the fibrotic group, indicating inflammatory activation of fibroblasts by TGF-β1 (Figure 21). To assess the effect on expression on Wnt signaling components, several components of the Wnt signaling pathway were investigated under stimulation with TGF-β1. Interestingly, the fibrotic fibroblasts displayed increased expression of the Wnt target gene Axin2 indicating activated Wnt-singaling under stimulation with TGF-β. Nevertheless, the non-fibrotic fibroblasts showed decreased expression of the secreted Wnt inhibitor SFRP4 (Figure 21). Importantly, we also found significantly upregulated expression of WISP-1 following TGF-β1-treatment. Taken together, we saw that stimulation with TGF-β1 induced pro-inflammatory state of the cells, indicated by increased expression of IL-6, and led to activation of Wnt signaling and expression of WISP-1 within the fibroblasts.

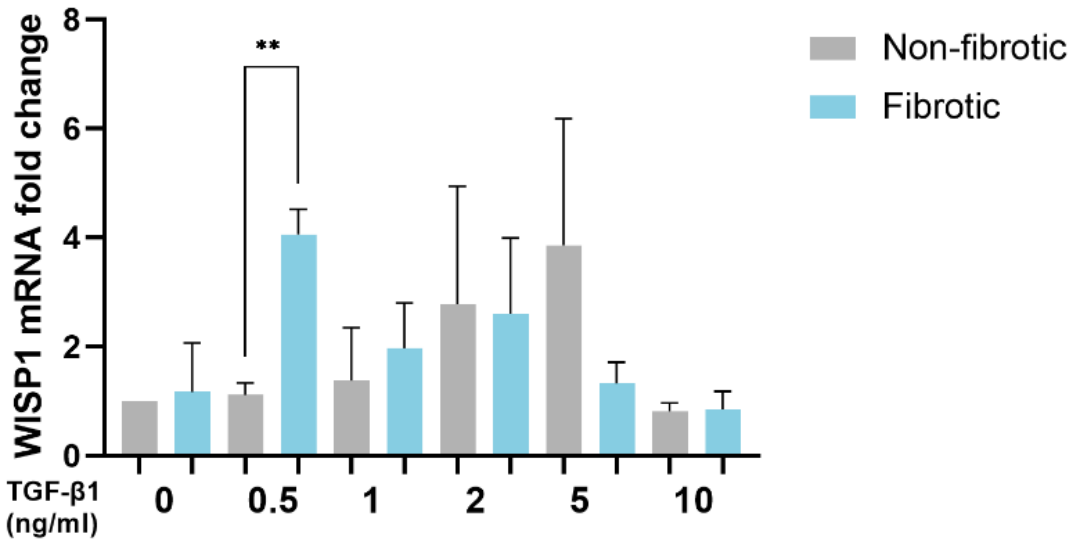

Figure 20. Fibroblasts were treated with increasing concentrations of TGF-β1 (0, 0.5, 1, 2, 5, 10 ng/ml) for 24h. WISP-1 mRNA expression levels were determined by qRT-PCR and normalized to hPPIB(*p < 0.05; **p < 0.01; *** p< 0.001; **** p< 0.0001; n=3).

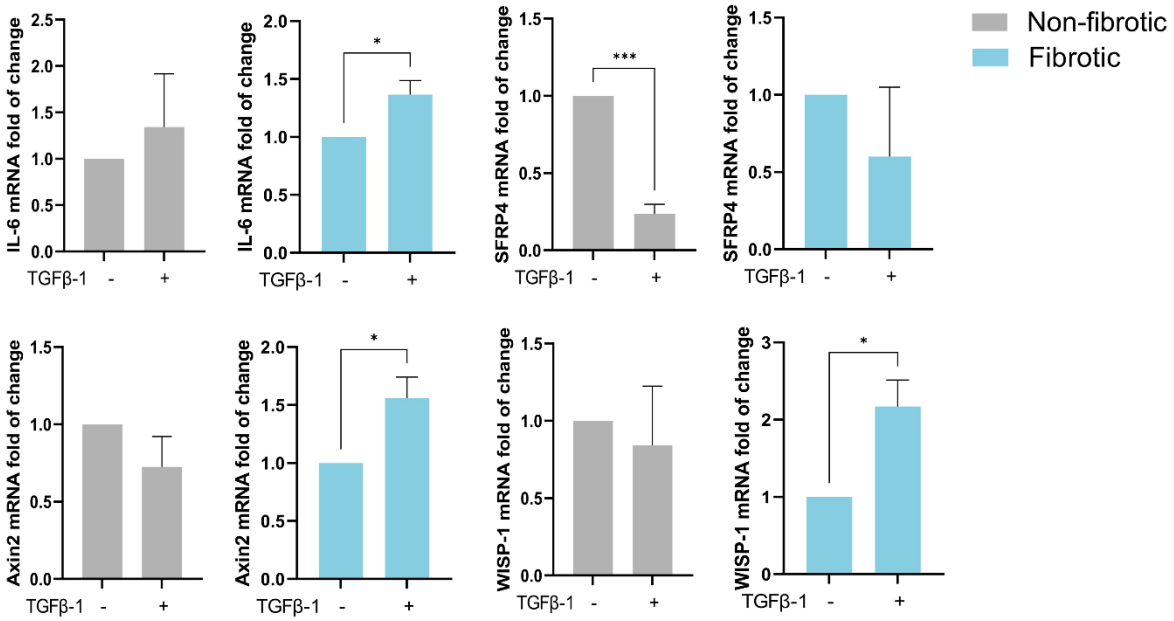

Figure 21. Gene expression of key components of Wnt/β-catenin signaling pathway including SFRP4, AXIN2, WISP-1 and IL-6 were analyzed by RT-qPCR. HPIFs were treated with TGF-β1 (0.5ng/ml) for 24h. Results are presented as mean ± SEM relative gene expression normalized to hPPIB and untreated fibroblasts (*p < 0.05; **p < 0.01; *** p< 0.001; **** p< 0.0001; n=3).

3.6 Treatment of rhWISP-1 promotes fibroblasts migration

3.6.1 Analysis of cell migration

Since we have found significantly increased expression of WISP-1 both in the human samples of intestinal fibrosis as well as under stimulation of primary human fibroblasts, we investigated whether WISP-1 had a stimulatory effect on intestinal fibroblasts perse. Thus, functional analyses were performed to assess cell migration as well as proliferation under stimulation with recombinant human WISP-1 (rhWISP-1). Regarding cell migration, scratch distances and width closure was obtained by comparison between images from time 0 to 24h under treatment with different concentration of rhWISP-1. Migration distances are shown separately during 0-6h, 6-12h and 12-24h. We observed that after 24h, the fibrotic fibroblasts

migrated faster than non-fibrotic fibroblasts under treatment with 40ng/ml rhWISP-1(Figure 22).

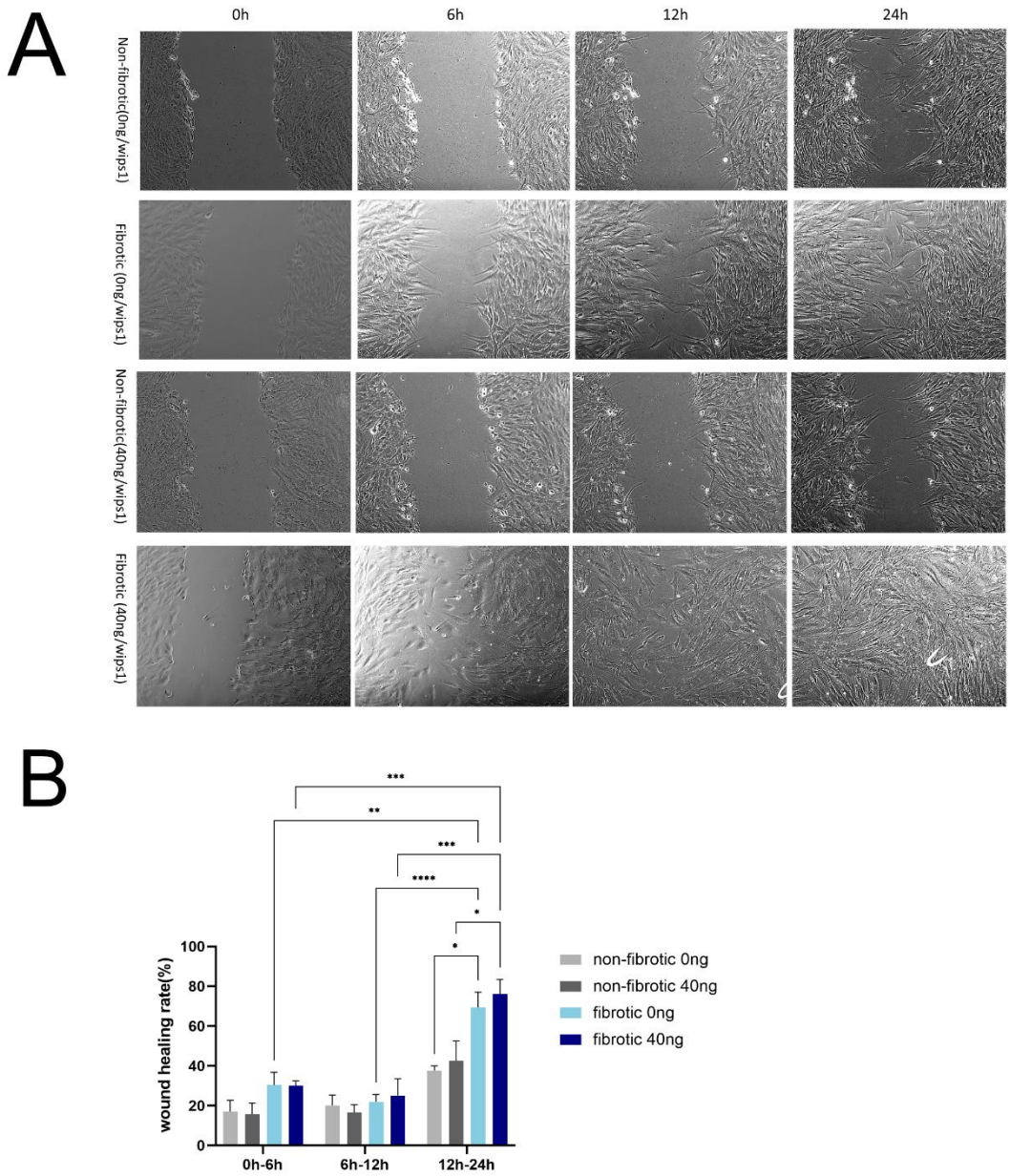

Figure 22. Effects of increasing doses of treatment with rhWISP-1 on the migration of HPIFs. (A) Representative images from in vitro scratch wound healing assays were recorded 0h, 6h, 12h, 24h after wounding. Scale bar: 50 μm. (B) Quantification of wound area invaded during 24h by untreated fibroblasts and fibroblasts treated with hWISP-1. The data are presented as mean ± SEM with the statistical significance levels (*p < 0.05; **p < 0.01; *** p< 0.001; **** p< 0.0001; n=3).

3.6.2 Analysis of cell proliferation

For assessment of migration wound healing assay and for measurement of cell proliferation MTT cell viability assays were performed. As depicted in Figure 23, proliferation increased under stimulation with WISP-1 but then again decreased under increasing concentrations, thus showing only a limited overall effect on cell proliferation.

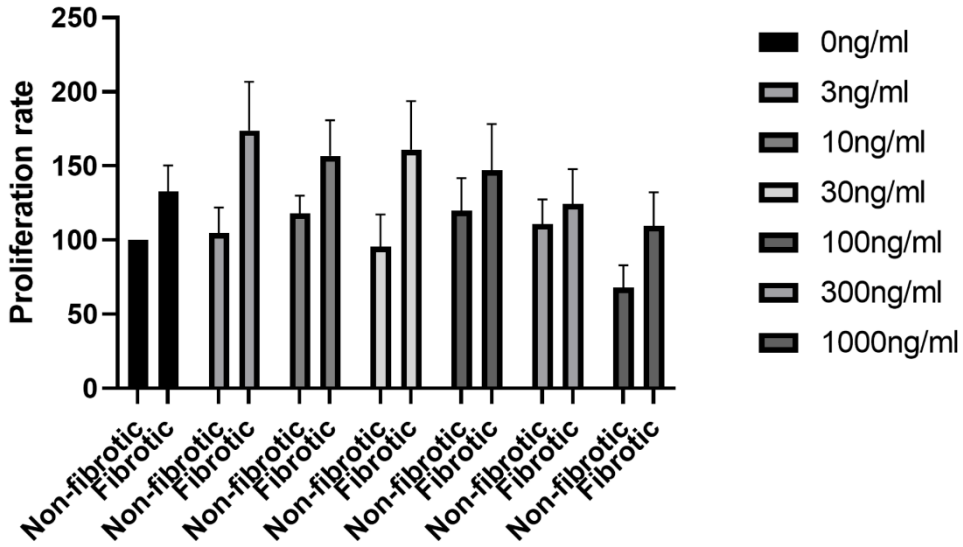

Figure 23. Analysis of fibroblasts proliferation after hWISP-1 treatment by in vitro MTT assay. The optical density (OD) data were plotted 24 hours following treatment with HPIFs rhWISP-1(30ng/ml) at progressively higher concentrations. The data are presented as mean ± SEM with the statistical significance levels (*p < 0.05; **p < 0.01; *** p< 0.001; **** p< 0.0001; n=3).

4. Discussion

4.1 WISP-1 is upregulated in intestinal fibrosis

Intestinal fibrosis is a serious complication in patients with CD. As a result of chronic inflammation, the wound healing process is impaired, resulting in the excessive deposition of ECM in the intestinal tract and thus a state of transmural disease[152]. Regardless of the morphology or histopathology (H&E, Sirius red, and Masson trichrome staining), presence of intestinal luminal narrowing induced by thickening of the bowel wall cannot be ignored.

The process of fibrogenesis and stricture formation is explained in the following manner. Several genes associated with CD risk have been identified by genome-wide association studies, including *WISP-1, LEF1, WNT3A, and WNT8A*. It is worth noticing that WISP-1, also known as CCN4/ELM-1 or WNT1-inducible signaling pathway protein 1, is an extracellular matrix-related protein. Recently, studies have demonstrated that WISP-1 is upregulated in human fibrotic organs such as lung, liver, kidney, and ligamentum flavum and associated with fibrosis[76, 91, 148, 153]. It has been reported that a high level of mechanical stress can induce the expression of WISP-1 during fibrogenesis. Through Hedgehog signaling, WISP-1 promoted the expression of fibrotic genes. This suggests a new axis of profibrotic signaling involving mechanical stress, WISP-1, and Hedgehog[153]. The involvement of WISP-1 in intestinal wound closure and inflammation has recently been demonstrated and previous research has suggested that some CCN family members including CCN1, CCN2, CCN4 may influence wound healing in fibrosis [154-157]. According to previous reports, an injury to the mucosa of the intestinal tract is associated with WISP-1 release and an increase in WISP-1 levels in colonic wound healing [80]. However, little is known about its possible implications in development of intestinal fibrosis in CD. In this study, we now, for the first time, report the novel observations that WISP-1 expression is increased in fibrotic regions in CD. WISP-1 mRNA expression is increased in fibrotic tissue and positively correlated with the severity of CD fibrosis. Our findings are consistent with other publications reporting increased WISP-1 levels in fibrotic organs, including the

liver, lung, and heart[76, 158, 159]. Therefore, WISP-1 may serve as a biomarker of intestinal fibrosis.

4.2 The role of human primary intestinal fibroblasts alterations in behaviour and ECM remodeling

Intestinal fibrosis is caused by the abnormal function of activated intestinal mesenchymal cells (proliferation, migration, contraction, ECM production), also known as myofibroblasts. Fibroblast plays a crucial role in the fibrosis process and also aids in wound healing[160-162]. When tissue is injured, fibroblasts differentiate into myofibroblasts and contribute to wound healing[163]. Healing wounds and inflammatory disorders are affected by sufficient fibroblast proliferation and migration. However, excessive fibroblast proliferation and migration may result in complications such as fibrosis[164]. Here, we discuss the types of fibroblasts and activation states involved in physiological and pathological repair, as well as their interactions with inflammation. Fibroblasts in our analysis prevailed this active state even after being passaged in culture conditions, which was evident in the migration and proliferation assays. This might be connected to epigenetic phenomenons or other changes on a molecular level that keep the cells in an activated state even without their original fibrotic environment. Inflammation, proliferation, and remodeling are all overlapping phases of normal repair[165, 166]. A key component of normal and pathological repair is the activation of fibroblasts for the creation of mechanically stable scar tissue from collagen-rich ECM[167]. Activation of fibroblasts can affect a variety of functions, including proliferation, migration, secretion activity, collagen production, and ECM remodeling[168, 169]. During the proliferative phase, fibroblasts multiply and migrate toward the wound area, increasing the synthesis of ECM(collagen, fibronectin, vimentin, timp1)[170]. Valeria et al. further showed that fibroblasts are activated as a result of inflammation *in vivo*; isolated fibroblasts retain this activation status because of autocrine stimulation (e.g. of growth factors), altered ECM, and intrinsic epigenetic reprogramming[169].

4.3 TGF-β1 regulates Wnt-signaling

While fibroblasts and myofibroblasts produce the majority of the extracellular matrix, new evidence suggests that gut obstruction can occur in a number of ways[171]. In the multifactorial environment in the fibrotic tissue not only inflammatory cells but also cytokines expressed from these cells directly influence fibroblast activity[172]. Cytokines such as transforming growth factor (TGF)-β play an important role in progression of fibrosis in the intestine and other organs[151, 173]. In this context, TGF-β1 regulates the phenotype and function of fibroblasts, such as cell differentiation into myofibroblasts and ECM deposition, and thus plays an important role in fibrogenesis. We found that stimulation of the fibroblasts with TGF-β1 promoted the expression of IL-6, which is one of the main cytokines involved in fibrogenesis. The same regulation has been demonstrated in primary human lung fibroblasts[174]. Myofibroblast biology was first implicated in WNT about 20 years ago[175]. There are two major Wnt signalling pathways: a canonical one (Wnt/β-catenin) and a non-canonical one (Wnt/Ca^{2+} and planar cell polarity (PCP))[176]. In accordance with their downstream signaling effects, Wnt proteins are classified as canonical (Wnt1, 2, 3, 8a, 8b, 10a, 10b) and non-canonical (Wnt4, 5a, 5b, 6, 7a, 7b and 11)[177]. TGF-β1 also exhibits numerous biological activities through activation of the canonical Wnt-signaling pathway, among which, WISP-1 has been reported to be associated with the action of TGF-β1[92]. This goes along with our observation that stimulation with TGF-β1 leads to significant induction of WISP-1 expression in intestinal fibroblasts. In addition to WISP-1, TGF-β1 partially reversed the inhibitory effects of rosiglitazone on Axin2 and β-catenin expression[178]. The downstream targets Axin2 showed similar results in our study. Secreted Frizzled Receptor Protein 4(SFRP4) is a member of a five-member family of extracellular proteins that functions as a repressor of Wnt signaling in cells[179-181]. It has been shown that SFRP4 recombinant protein reduces renal levels of β-catenin protein and increases phosphorylated β-catenin signaling when the protein is infused into rats[182]. However, the expression of skin fibrosis-associated protein 4 in hypodermal connective tissues and fascia between the skin and skeletal muscle is selectively increased in skin fibrosis mouse models[179]. It may be possible that increased SFRP4 is a counter-regulatory mechanism for Wnt activity in these reverse data. Taken together, these results showed modulation of fibrosis-related genes including

WISP-1, Axin2, and SFRP4 supporting the conclusion of ongoing Wnt activity and up-regulation of fibrosis signature genes in response to TGF-β1 stimulation.

4.4 WISP-1 affects fibroblast migration

The Wnt pathway regulates a number of genes, including WISP-1, which is known to modulate vascular smooth muscle cell (VSMC) migration[183]. WISP-1 interacts with integrins to promote VSMC migration, as well[183]. WISP-1 not only acts in VSMC but also enhances cancer cell migration[184]. WISP-1 knockdown decreased proliferation, migration, and invasion in two cell lines expressing high levels of endogenous WISP-1[185]. To examine the effect of WISP-1 on fibroblasts we stimulated the cells with recombinant human WISP-1 and found enhanced migratory activity under stimulation. During skin wound healing, WISP-1 is upregulated during dermal fibroblast migration, which is consistent with its role in normal physiology in fibroblasts[103]. Mitsuaki et al. reported that WISP-1 affects wound healing through its functions in regulating migration of dermal fibroblasts via integrin α5β1 signaling[103]. WISP-1 control the migration of fibroblast suggesting that WISP-1 could enhance cell mobility in a similar way. Importantly, stimulation of primary human fibroblasts with WISP-1 in turn facilitated directed cell migration in vitro which might ultimately contribute to fibrosis formation. Therefore, WISP-1/CCN4 may be used for wound healing in the future.

Although the proliferation of fibroblasts in strictures is increased compared to controls, no significant difference in the proliferation was found under treatment with WISP-1, suggesting that WISP-1 had no specific effect on stimulating fibroblast proliferation. That might be expla`ined by domain-specific biological functions of CCN protein and reactivity of different cell types. The N-terminal domain of CCN2 mediates migration in myofibroblasts, while the C-terminal domain mediates proliferation[186]. WISP-1 promoted morphological transformation, accelerated cell proliferation, and increased saturation density in normal rat kidney fibroblasts, while Hashimoto et al. found that a mouse orthologue of WISP-1 suppressed melanoma growth[56, 187]. Therefore, the proliferation-controlling domain of WISP-1 may not be responsive to intestinal fibroblasts.

Taken together, the present data reveal a contribution of WISP-1 to the

pathogenesis of CD fibrosis. While in our study WISP-1 has been studied in collected human specimens and primary cells, more mechanistic insights will be gained from animal studies in the future.

5. Summary

In conclusion, in accordance with microarray analysis, a definite set of Wnt-signaling components (including Wnt3a, Wnt2, Wnt8a, MMP7, LEF1 and WISP-1) was found to be significantly upregulated during the fibrosis stage of CD. Our attention was further piqued by the following: WISP-1 was upregulated 2x fold compared to non-fibrotic control tissue. In order to validate this upregulation, surgical specimens of Crohn's disease with fibrotic features were obtained. Fibrotic sections were characterized by massive hypertrophy (an increase in volume) of the muscularis propria smooth muscle, hyperplasia of the smooth muscle, and a replacement of the typical loose connective tissue. Compared to the control group, the fibrotic group exhibits an increase in collagen deposition that is notable compared to the control group. As a result of the study, we observed that the fibrotic score was highly correlated with the pathological classification.

Next, it has been demonstrated that the primary fibroblasts isolated from intestinal tissue of CD patients are consistently positive for a-SMA and vimentin. This result indicates that the isolated primary intestinal fibroblasts are all activated myofibroblasts. There was a significant difference between the ECM synthesis (Col1A1, Vimentin, Fibronectin, and TIMP1) and degradation responses of different fibroblast types. During the course of the study, significant differences were observed between the control and fibrosis groups in terms of cell proliferation and migration. The fact that TGF-β1 is able to activate the Wnt signalling pathway and the expression of WISP-1 is of importance. The final result of our study is that WISP-1 stimulates fibroblast migration but does not affect fibroblast proliferation in any way.

Taken together we could show increased expression of WISP-1 in fibrotic CD with an effect on enhancing fibroblast motility and thereby enhancing fibrogenesis, potentially mediated through TGF-β1 signaling. Our data indicates a strong potential of anti-WISP-1 treatment in prevention of fibrogenesis in CD.

6. Zusammenfassung

In Übereinstimmung mit der Microarray-Analyse wurde festgestellt, dass eine Reihe von Wnt-Signalkomponenten (einschließlich Wnt3a, Wnt2, Wnt8a, MMP7, LEF1 und WISP-1) während des Fibrosestadiums der CD signifikant hochreguliert sind. Unsere Aufmerksamkeit wurde durch Folgendes weiter gesteigert: WISP-1 war im Vergleich zu nicht-fibrotischem Kontrollgewebe um das Zweifache hochreguliert. Um diese Hochregulierung zu bestätigen, wurden chirurgische Präparate von Morbus Crohn mit fibrotischen Merkmalen entnommen. Fibrotische Schnitte waren durch eine massive Hypertrophie (Volumenzunahme) der glatten Muskulatur der Muscularis propria, eine Hyperplasie der glatten Muskulatur und einen Ersatz des typischen lockeren Bindegewebes gekennzeichnet. Im Vergleich zur Kontrollgruppe weist die fibrotische Gruppe eine auffällige Zunahme der Kollagenablagerung auf. Als Ergebnis der Studie stellten wir fest, dass der Fibrotik-Score stark mit der pathologischen Klassifizierung korreliert war.

Außerdem wurde nachgewiesen, dass die aus dem Darmgewebe von CD-Patienten isolierten primären Fibroblasten durchweg positiv für a-SMA und Vimentin sind. Dieses Ergebnis deutet darauf hin, dass die isolierten primären Darmfibroblasten alle aktivierte Myofibroblasten sind. Es gab einen signifikanten Unterschied zwischen der ECM-Synthese (Col1A1, Vimentin, Fibronectin und TIMP1) und den Abbau-Reaktionen der verschiedenen Fibroblastentypen. Im Verlauf der Studie wurden signifikante Unterschiede zwischen der Kontroll- und der Fibrosegruppe in Bezug auf die Zellproliferation und -migration festgestellt. Die Tatsache, dass TGF-β1 in der Lage ist, den Wnt-Signalweg und die Expression von WISP-1 zu aktivieren, ist von Bedeutung. Das Endergebnis unserer Studie ist, dass WISP-1 die Fibroblastenmigration stimuliert, aber die Fibroblastenproliferation in keiner Weise beeinflusst.

Insgesamt konnten wir eine erhöhte Expression von WISP-1 in der fibrotischen CD nachweisen, die die Fibroblastenmotilität und damit die Fibrogenese fördert, was möglicherweise durch TGF-β1-Signale vermittelt wird. Unsere Daten deuten auf ein großes Potenzial der Anti-WISP-1-Behandlung bei der Prävention der Fibrogenese bei CD hin.

7. References

1. Ananthakrishnan AN. Epidemiology and risk factors for IBD. Nat Rev Gastroenterol Hepatol 2015;12:205-17.
2. Rieder F, Zimmermann EM, Remzi FH, et al. Crohn's disease complicated by strictures: a systematic review. Gut 2013;62:1072-84.
3. Nos P, Domenech E. Postoperative Crohn's disease recurrence: a practical approach. World J Gastroenterol 2008;14:5540-8.
4. Santacroce G, Lenti MV, Di Sabatino A. Therapeutic Targeting of Intestinal Fibrosis in Crohn's Disease. Cells 2022;11:429.
5. Gionchetti P, Dignass A, Danese S, et al. 3rd European Evidence-based Consensus on the Diagnosis and Management of Crohn's Disease 2016: Part 2: Surgical Management and Special Situations. J Crohns Colitis 2017;11:135-149.
6. Lichtenstein GR, Loftus EV, Isaacs KL, et al. ACG Clinical Guideline: Management of Crohn's Disease in Adults. Am J Gastroenterol 2018;113:481-517.
7. Satsangi J, Silverberg MS, Vermeire S, et al. The Montreal classification of inflammatory bowel disease: controversies, consensus, and implications. Gut 2006;55:749-53.
8. Chan WPW, Mourad F, Leong RW. Crohn's disease associated strictures. J Gastroenterol Hepatol 2018;33:998-1008.
9. Panes J, Bouzas R, Chaparro M, et al. Systematic review: the use of ultrasonography, computed tomography and magnetic resonance imaging for the diagnosis, assessment of activity and abdominal complications of Crohn's disease. Alimentary Pharmacology & Therapeutics 2011;34:125-145.
10. Daperno M, D'Haens G, Van Assche G, et al. Development and validation of a new, simplified endoscopic activity score for Crohn's disease: the SES-CD. Gastrointest Endosc 2004;60:505-12.
11. Rieder F, Fiocchi C, Rogler G. Mechanisms, Management, and Treatment of Fibrosis in Patients With Inflammatory Bowel Diseases. Gastroenterology 2017;152:340-350 e6.
12. Thia KT, Sandborn WJ, Harmsen WS, et al. Risk factors associated with progression to intestinal complications of Crohn's disease in a population-based cohort. Gastroenterology 2010;139:1147-55.
13. Sadler T, Bhasin JM, Xu Y, et al. Genome-wide analysis of DNA methylation and gene expression defines molecular characteristics of Crohn's disease-associated fibrosis. Clin Epigenetics 2016;8:30.
14. Raghu G, Brown KK, Costabel U, et al. Treatment of idiopathic pulmonary fibrosis with etanercept: an exploratory, placebo-controlled trial. Am J Respir Crit Care Med 2008;178:948-55.
15. Horton MR, Santopietro V, Mathew L, et al. Thalidomide for the treatment of cough in idiopathic pulmonary fibrosis: a randomized trial. Ann Intern Med 2012;157:398-406.
16. Zhang X, Ko HM, Torres J, et al. Luminally polarized mural and vascular remodeling in ileal strictures of Crohn's disease. Hum Pathol 2018;79:42-49.

17. Graham MF, Diegelmann RF, Elson CO, et al. Collagen content and types in the intestinal strictures of Crohn's disease. Gastroenterology 1988;94:257-65.
18. Li J, Mao R, Kurada S, et al. Pathogenesis of fibrostenosing Crohn's disease. Transl Res 2019;209:39-54.
19. Rieder F, Brenmoehl J, Leeb S, et al. Wound healing and fibrosis in intestinal disease. Gut 2007;56:130-9.
20. Meijer MJ, Mieremet-Ooms MA, van der Zon AM, et al. Increased mucosal matrix metalloproteinase-1, -2, -3 and -9 activity in patients with inflammatory bowel disease and the relation with Crohn's disease phenotype. Dig Liver Dis 2007;39:733-9.
21. McKaig BC, McWilliams D, Watson SA, et al. Expression and regulation of tissue inhibitor of metalloproteinase-1 and matrix metalloproteinases by intestinal myofibroblasts in inflammatory bowel disease. Am J Pathol 2003;162:1355-60.
22. Pinchuk IV, Powell DW. Immunosuppression by Intestinal Stromal Cells. Adv Exp Med Biol 2018;1060:115-129.
23. Baum J, Duffy HS. Fibroblasts and myofibroblasts: what are we talking about? J Cardiovasc Pharmacol 2011;57:376-9.
24. de Bruyn JR, van den Brink GR, Steenkamer J, et al. Fibrostenotic Phenotype of Myofibroblasts in Crohn's Disease is Dependent on Tissue Stiffness and Reversed by LOX Inhibition. J Crohns Colitis 2018;12:849-859.
25. Wynn TA. Cellular and molecular mechanisms of fibrosis. J Pathol 2008;214:199-210.
26. Speca S, Giusti I, Rieder F, et al. Cellular and molecular mechanisms of intestinal fibrosis. World J Gastroenterol 2012;18:3635-61.
27. Wynn TA, Ramalingam TR. Mechanisms of fibrosis: therapeutic translation for fibrotic disease. Nat Med 2012;18:1028-40.
28. Ng EK, Panesar N, Longo WE, et al. Human intestinal epithelial and smooth muscle cells are potent producers of IL-6. Mediators Inflamm 2003;12:3-8.
29. Koukoulis G, Ke Y, Henley JD, et al. Obliterative muscularization of the small bowel submucosa in Crohn disease: a possible mechanism of small bowel obstruction. Arch Pathol Lab Med 2001;125:1331-4.
30. Sheehan AL, Warren BF, Gear MW, et al. Fat-wrapping in Crohn's disease: pathological basis and relevance to surgical practice. Br J Surg 1992;79:955-8.
31. Westcott E, Windsor A, Mattacks C, et al. Fatty acid compositions of lipids in mesenteric adipose tissue and lymphoid cells in patients with and without Crohn's disease and their therapeutic implications. Inflammatory Bowel Diseases 2005;11:820-827.
32. Rieder F. Managing Intestinal Fibrosis in Patients With Inflammatory Bowel Disease. Gastroenterol Hepatol (N Y) 2018;14:120-122.
33. Ray S, De Salvo C, Pizarro TT. Central role of IL-17/Th17 immune responses and the gut microbiota in the pathogenesis of intestinal fibrosis. Curr Opin Gastroenterol 2014;30:531-8.
34. Maddur MS, Miossec P, Kaveri SV, et al. Th17 cells: biology, pathogenesis of autoimmune and inflammatory diseases, and therapeutic strategies. Am J Pathol 2012;181:8-18.
35. Fujino S, Andoh A, Bamba S, et al. Increased expression of interleukin 17 in inflammatory bowel disease. Gut 2003;52:65-70.

36. Holtta V, Klemetti P, Sipponen T, et al. IL-23/IL-17 immunity as a hallmark of Crohn's disease. Inflamm Bowel Dis 2008;14:1175-84.
37. Biancheri P, Pender SL, Ammoscato F, et al. The role of interleukin 17 in Crohn's disease-associated intestinal fibrosis. Fibrogenesis Tissue Repair 2013;6:13.
38. Higgins DP, Hemsley S, Canfield PJ. Association of uterine and salpingeal fibrosis with chlamydial hsp60 and hsp10 antigen-specific antibodies in Chlamydia-infected koalas. Clin Diagn Lab Immunol 2005;12:632-9.
39. Fehrenbach H, Wagner C, Wegmann M. Airway remodeling in asthma: what really matters. Cell Tissue Res 2017;367:551-569.
40. Bailey JR, Bland PW, Tarlton JF, et al. IL-13 promotes collagen accumulation in Crohn's disease fibrosis by down-regulation of fibroblast MMP synthesis: a role for innate lymphoid cells? PLoS One 2012;7:e52332.
41. Lee CG, Homer RJ, Zhu Z, et al. Interleukin-13 induces tissue fibrosis by selectively stimulating and activating transforming growth factor beta(1). J Exp Med 2001;194:809-21.
42. Fichtner-Feigl S, Fuss IJ, Young CA, et al. Induction of IL-13 triggers TGF-beta1-dependent tissue fibrosis in chronic 2,4,6-trinitrobenzene sulfonic acid colitis. J Immunol 2007;178:5859-70.
43. Salvador P, Macias-Ceja DC, Gisbert-Ferrandiz L, et al. CD16+ Macrophages Mediate Fibrosis in Inflammatory Bowel Disease. J Crohns Colitis 2018;12:589-599.
44. Wynn TA, Vannella KM. Macrophages in Tissue Repair, Regeneration, and Fibrosis. Immunity 2016;44:450-462.
45. Wilson MS, Elnekave E, Mentink-Kane MM, et al. IL-13Ralpha2 and IL-10 coordinately suppress airway inflammation, airway-hyperreactivity, and fibrosis in mice. J Clin Invest 2007;117:2941-51.
46. Seki E, De Minicis S, Osterreicher CH, et al. TLR4 enhances TGF-beta signaling and hepatic fibrosis. Nat Med 2007;13:1324-32.
47. Uehara A, Takada H. Functional TLRs and NODs in human gingival fibroblasts. J Dent Res 2007;86:249-54.
48. Otte JM, Rosenberg IM, Podolsky DK. Intestinal myofibroblasts in innate immune responses of the intestine. Gastroenterology 2003;124:1866-78.
49. Shelley-Fraser G, Borley NR, Warren BF, et al. The connective tissue changes of Crohn's disease. Histopathology 2012;60:1034-44.
50. Flier SN, Tanjore H, Kokkotou EG, et al. Identification of epithelial to mesenchymal transition as a novel source of fibroblasts in intestinal fibrosis. J Biol Chem 2010;285:20202-12.
51. Lawrance IC, Maxwell L, Doe W. Altered response of intestinal mucosal fibroblasts to profibrogenic cytokines in inflammatory bowel disease. Inflamm Bowel Dis 2001;7:226-36.
52. Rieder F, Kessler SP, West GA, et al. Inflammation-induced endothelial-to-mesenchymal transition: a novel mechanism of intestinal fibrosis. Am J Pathol 2011;179:2660-73.
53. Bettenworth D, Rieder F. Medical therapy of stricturing Crohn's disease: what the gut can learn from other organs - a systematic review. Fibrogenesis & Tissue Repair 2014;7:5.
54. Beddy D, Mulsow J, Watson RW, et al. Expression and regulation of connective tissue growth factor by transforming growth factor beta and tumour necrosis factor alpha in fibroblasts isolated from strictures in patients

with Crohn's disease. Br J Surg 2006;93:1290-6.
55. Medina C, Santos-Martinez MJ, Santana A, et al. Transforming growth factor-beta type 1 receptor (ALK5) and Smad proteins mediate TIMP-1 and collagen synthesis in experimental intestinal fibrosis. J Pathol 2011;224:461-72.
56. Hashimoto Y, Shindo-Okada N, Tani M, et al. Expression of the Elm1 gene, a novel gene of the CCN (connective tissue growth factor, Cyr61/Cef10, and neuroblastoma overexpressed gene) family, suppresses In vivo tumor growth and metastasis of K-1735 murine melanoma cells. J Exp Med 1998;187:289-96.
57. Jun JI, Lau LF. Taking aim at the extracellular matrix: CCN proteins as emerging therapeutic targets. Nature Reviews Drug Discovery 2011;10:945-963.
58. Chen CC, Lau LF. Functions and mechanisms of action of CCN matricellular proteins. Int J Biochem Cell Biol 2009;41:771-83.
59. Pennica D, Swanson TA, Welsh JW, et al. WISP genes are members of the connective tissue growth factor family that are up-regulated in Wnt-1-transformed cells and aberrantly expressed in human colon tumors. Proceedings of the National Academy of Sciences of the United States of America 1998;95:14717-14722.
60. Brigstock DR, Goldschmeding R, Katsube KI, et al. Proposal for a unified CCN nomenclature. Mol Pathol 2003;56:127-8.
61. Berschneider B, Konigshoff M. WNT1 inducible signaling pathway protein 1 (WISP1): a novel mediator linking development and disease. Int J Biochem Cell Biol 2011;43:306-9.
62. Feng M, Jia S. Dual effect of WISP-1 in diverse pathological processes. Chin J Cancer Res 2016;28:553-560.
63. Mancuso DJ, Tuley EA, Westfield LA, et al. Structure of the gene for human von Willebrand factor. J Biol Chem 1989;264:19514-27.
64. Hashimoto G, Inoki I, Fujii Y, et al. Matrix metalloproteinases cleave connective tissue growth factor and reactivate angiogenic activity of vascular endothelial growth factor 165. J Biol Chem 2002;277:36288-95.
65. Holt GD, Pangburn MK, Ginsburg V. Properdin binds to sulfatide [Gal(3-SO4)beta 1-1 Cer] and has a sequence homology with other proteins that bind sulfated glycoconjugates. J Biol Chem 1990;265:2852-5.
66. Voorberg J, Fontijn R, Calafat J, et al. Assembly and routing of von Willebrand factor variants: the requirements for disulfide-linked dimerization reside within the carboxy-terminal 151 amino acids. J Cell Biol 1991;113:195-205.
67. Tanaka S, Sugimachi K, Saeki H, et al. A novel variant of WISP1 lacking a Von Willebrand type C module overexpressed in scirrhous gastric carcinoma. Oncogene 2001;20:5525-32.
68. Yanagita T, Kubota S, Kawaki H, et al. Expression and physiological role of CCN4/Wnt-induced secreted protein 1 mRNA splicing variants in chondrocytes. FEBS J 2007;274:1655-65.
69. Cervello M, Giannitrapani L, Labbozzetta M, et al. Expression of WISPs and of their novel alternative variants in human hepatocellular carcinoma cells. Signal Transduction and Communication in Cancer Cells 2004;1028:432-439.
70. French DM, Kaul RJ, D'Souza AL, et al. WISP-1 is an osteoblastic regulator

expressed during skeletal development and fracture repair. American Journal of Pathology 2004;165:855-867.
71. Blom AB, Brockbank SM, van Lent PL, et al. Involvement of the Wnt signaling pathway in experimental and human osteoarthritis: prominent role of Wnt-induced signaling protein 1. Arthritis Rheum 2009;60:501-12.
72. Cheng C, Tian J, Zhang F, et al. WISP1 Protects Against Chondrocyte Senescence and Apoptosis by Regulating alphavbeta3 and PI3K/Akt Pathway in Osteoarthritis. DNA Cell Biol 2021;40:629-637.
73. Zhang Q, Zhang C, Li X, et al. WISP1 Is Increased in Intestinal Mucosa and Contributes to Inflammatory Cascades in Inflammatory Bowel Disease. Dis Markers 2016;2016:3547096.
74. Venkatachalam K, Venkatesan B, Valente AJ, et al. WISP1, a pro-mitogenic, pro-survival factor, mediates tumor necrosis factor-alpha (TNF-alpha)-stimulated cardiac fibroblast proliferation but inhibits TNF-alpha-induced cardiomyocyte death. J Biol Chem 2009;284:14414-27.
75. Chen H, Fan Y, Jing H, et al. LncRNA Gm12840 mediates WISP1 to regulate ischemia-reperfusion-induced renal fibrosis by sponging miR-677-5p. Epigenomics 2020;12:2205-2218.
76. Konigshoff M, Kramer M, Balsara N, et al. WNT1-inducible signaling protein-1 mediates pulmonary fibrosis in mice and is upregulated in humans with idiopathic pulmonary fibrosis. J Clin Invest 2009;119:772-87.
77. Fernandez-Ruiz R, Garcia-Alaman A, Esteban Y, et al. Wisp1 is a circulating factor that stimulates proliferation of adult mouse and human beta cells. Nat Commun 2020;11:5982.
78. Basak S, Sarkar A, Mathapati S, et al. Cellular growth and tube formation of HTR8/SVneo trophoblast: effects of exogenously added fatty acid-binding protein-4 and its inhibitor. Mol Cell Biochem 2018;437:55-64.
79. Sahin Ersoy G, Altun Ensari T, Vatansever D, et al. Novel adipokines WISP1 and betatrophin in PCOS: relationship to AMH levels, atherogenic and metabolic profile. Gynecol Endocrinol 2017;33:119-123.
80. Quiros M, Nishio H, Neumann PA, et al. Macrophage-derived IL-10 mediates mucosal repair by epithelial WISP-1 signaling. J Clin Invest 2017;127:3510-3520.
81. Katoh Y, Katoh M. Conserved POU-binding site linked to SP1-binding site within FZD5 promoter: Transcriptional mechanisms of FZD5 in undifferentiated human ES cells, fetal liver/spleen, adult colon, pancreatic islet, and diffuse-type gastric cancer. Int J Oncol 2007;30:751-5.
82. Xie D, Nakachi K, Wang H, et al. Elevated levels of connective tissue growth factor, WISP-1, and CYR61 in primary breast cancers associated with more advanced features. Cancer Res 2001;61:8917-23.
83. Bizama C, Benavente F, Salvatierra E, et al. The low-abundance transcriptome reveals novel biomarkers, specific intracellular pathways and targetable genes associated with advanced gastric cancer. Int J Cancer 2014;134:755-64.
84. Cao D, Hustinx SR, Sui G, et al. Identification of novel highly expressed genes in pancreatic ductal adenocarcinomas through a bioinformatics analysis of expressed sequence tags. Cancer Biol Ther 2004;3:1081-9; discussion 1090-1.
85. Chuang JY, Chang AC, Chiang IP, et al. Apoptosis signal-regulating kinase 1 is involved in WISP-1-promoted cell motility in human oral squamous cell

carcinoma cells. PLoS One 2013;8:e78022.
86. Chen PP, Li WJ, Wang Y, et al. Expression of Cyr61, CTGF, and WISP-1 correlates with clinical features of lung cancer. PLoS One 2007;2:e534.
87. Davies SR, Davies ML, Sanders A, et al. Differential expression of the CCN family member WISP-1, WISP-2 and WISP-3 in human colorectal cancer and the prognostic implications. Int J Oncol 2010;36:1129-36.
88. Gurbuz I, Chiquet-Ehrismann R. CCN4/WISP1 (WNT1 inducible signaling pathway protein 1): a focus on its role in cancer. Int J Biochem Cell Biol 2015;62:142-6.
89. Berschneider B, Ellwanger DC, Baarsma HA, et al. miR-92a regulates TGF-beta1-induced WISP1 expression in pulmonary fibrosis. Int J Biochem Cell Biol 2014;53:432-41.
90. Wang B, Ding X, Ding C, et al. WNT1-inducible-signaling pathway protein 1 regulates the development of kidney fibrosis through the TGF-beta1 pathway. FASEB J 2020;34:14507-14520.
91. Jian YC, Wang JJ, Dong S, et al. Wnt-induced secreted protein 1/CCN4 in liver fibrosis both in vitro and in vivo. Clin Lab 2014;60:29-35.
92. Klee S, Lehmann M, Wagner DE, et al. WISP1 mediates IL-6-dependent proliferation in primary human lung fibroblasts. Sci Rep 2016;6:20547.
93. Jia H, Janjanam J, Wu SC, et al. The tumor cell-secreted matricellular protein WISP1 drives pro-metastatic collagen linearization. EMBO J 2019;38:e101302.
94. Liu H, Dong W, Lin Z, et al. CCN4 regulates vascular smooth muscle cell migration and proliferation. Mol Cells 2013;36:112-8.
95. Hou CH, Chiang YC, Fong YC, et al. WISP-1 increases MMP-2 expression and cell motility in human chondrosarcoma cells. Biochem Pharmacol 2011;81:1286-95.
96. Stephens S, Palmer J, Konstantinova I, et al. A functional analysis of Wnt inducible signalling pathway protein -1 (WISP-1/CCN4). J Cell Commun Signal 2015;9:63-72.
97. Polakis P. The oncogenic activation of beta-catenin. Curr Opin Genet Dev 1999;9:15-21.
98. Schlegelmilch K, Keller A, Zehe V, et al. WISP 1 is an important survival factor in human mesenchymal stromal cells. Gene 2014;551:243-54.
99. Jing D, Zhang Q, Yu H, et al. Identification of WISP1 as a novel oncogene in glioblastoma. Int J Oncol 2017;51:1261-1270.
100. Wu J, Long Z, Cai H, et al. High expression of WISP1 in colon cancer is associated with apoptosis, invasion and poor prognosis. Oncotarget 2016;7:49834-49847.
101. Ferrand N, Bereziat V, Moldes M, et al. WISP1/CCN4 inhibits adipocyte differentiation through repression of PPARgamma activity. Sci Rep 2017;7:1749.
102. Ma X, Wang D, Zhao W, et al. Deciphering the Roles of PPARgamma in Adipocytes via Dynamic Change of Transcription Complex. Front Endocrinol (Lausanne) 2018;9:473.
103. Ono M, Masaki A, Maeda A, et al. CCN4/WISP1 controls cutaneous wound healing by modulating proliferation, migration and ECM expression in dermal fibroblasts via alpha5beta1 and TNFalpha. Matrix Biol 2018;68-69:533-546.
104. Li Z, Dang J, Chang KY, et al. MicroRNA-mediated regulation of extracellular matrix formation modulates somatic cell reprogramming. RNA 2014;20:1900-

15.
105. Moses HL, Roberts AB, Derynck R. The Discovery and Early Days of TGF-beta: A Historical Perspective. Cold Spring Harb Perspect Biol 2016;8.
106. Morikawa M, Derynck R, Miyazono K. TGF-beta and the TGF-beta Family: Context-Dependent Roles in Cell and Tissue Physiology. Cold Spring Harb Perspect Biol 2016;8.
107. Dong X, Zhao B, Iacob RE, et al. Force interacts with macromolecular structure in activation of TGF-beta. Nature 2017;542:55-59.
108. Frangogiannis N. Transforming growth factor-beta in tissue fibrosis. J Exp Med 2020;217:e20190103.
109. Bellini A, Mattoli S. The role of the fibrocyte, a bone marrow-derived mesenchymal progenitor, in reactive and reparative fibroses. Lab Invest 2007;87:858-70.
110. Chiang HY, Chu PH, Lee TH. R1R2 peptide ameliorates pulmonary fibrosis in mice through fibrocyte migration and differentiation. PLoS One 2017;12:e0185811.
111. de Oliveira RC, Wilson SE. Fibrocytes, Wound Healing, and Corneal Fibrosis. Invest Ophthalmol Vis Sci 2020;61:28.
112. Lan HY. Diverse roles of TGF-beta/Smads in renal fibrosis and inflammation. Int J Biol Sci 2011;7:1056-67.
113. Sanjabi S, Zenewicz LA, Kamanaka M, et al. Anti-inflammatory and pro-inflammatory roles of TGF-beta, IL-10, and IL-22 in immunity and autoimmunity. Curr Opin Pharmacol 2009;9:447-53.
114. Dardalhon V, Awasthi A, Kwon H, et al. IL-4 inhibits TGF-beta-induced Foxp3+ T cells and, together with TGF-beta, generates IL-9+ IL-10+ Foxp3(-) effector T cells. Nat Immunol 2008;9:1347-55.
115. Veldhoen M, Uyttenhove C, van Snick J, et al. Transforming growth factor-beta 'reprograms' the differentiation of T helper 2 cells and promotes an interleukin 9-producing subset. Nat Immunol 2008;9:1341-6.
116. Monteleone G, Kumberova A, Croft NM, et al. Blocking Smad7 restores TGF-beta1 signaling in chronic inflammatory bowel disease. J Clin Invest 2001;108:601-9.
117. Di Sabatino A, Pickard KM, Rampton D, et al. Blockade of transforming growth factor beta upregulates T-box transcription factor T-bet, and increases T helper cell type 1 cytokine and matrix metalloproteinase-3 production in the human gut mucosa. Gut 2008;57:605-12.
118. Tsunawaki S, Sporn M, Ding A, et al. Deactivation of macrophages by transforming growth factor-beta. Nature 1988;334:260-2.
119. Chen B, Huang S, Su Y, et al. Macrophage Smad3 Protects the Infarcted Heart, Stimulating Phagocytosis and Regulating Inflammation. Circ Res 2019;125:55-70.
120. McDonald LT, Zile MR, Zhang Y, et al. Increased macrophage-derived SPARC precedes collagen deposition in myocardial fibrosis. Am J Physiol Heart Circ Physiol 2018;315:H92-H100.
121. Zeisberg M, Hanai J, Sugimoto H, et al. BMP-7 counteracts TGF-beta1-induced epithelial-to-mesenchymal transition and reverses chronic renal injury. Nat Med 2003;9:964-8.
122. Sato M, Muragaki Y, Saika S, et al. Targeted disruption of TGF-beta1/Smad3 signaling protects against renal tubulointerstitial fibrosis induced by unilateral ureteral obstruction. J Clin Invest 2003;112:1486-94.

123. Rygiel KA, Robertson H, Marshall HL, et al. Epithelial-mesenchymal transition contributes to portal tract fibrogenesis during human chronic liver disease. Lab Invest 2008;88:112-23.
124. Willis BC, Liebler JM, Luby-Phelps K, et al. Induction of epithelial-mesenchymal transition in alveolar epithelial cells by transforming growth factor-beta1: potential role in idiopathic pulmonary fibrosis. Am J Pathol 2005;166:1321-32.
125. Boor P, Ostendorf T, Floege J. Renal fibrosis: novel insights into mechanisms and therapeutic targets. Nat Rev Nephrol 2010;6:643-56.
126. Khalil H, Kanisicak O, Prasad V, et al. Fibroblast-specific TGF-beta-Smad2/3 signaling underlies cardiac fibrosis. J Clin Invest 2017;127:3770-3783.
127. Wei Y, Kim TJ, Peng DH, et al. Fibroblast-specific inhibition of TGF-beta1 signaling attenuates lung and tumor fibrosis. J Clin Invest 2017;127:3675-3688.
128. Tang PM, Nikolic-Paterson DJ, Lan HY. Macrophages: versatile players in renal inflammation and fibrosis. Nat Rev Nephrol 2019;15:144-158.
129. Hinz B, McCulloch CA, Coelho NM. Mechanical regulation of myofibroblast phenoconversion and collagen contraction. Exp Cell Res 2019;379:119-128.
130. Saadat S, Noureddini M, Mahjoubin-Tehran M, et al. Pivotal Role of TGF-beta/Smad Signaling in Cardiac Fibrosis: Non-coding RNAs as Effectual Players. Front Cardiovasc Med 2020;7:588347.
131. Zhang YE. Non-Smad Signaling Pathways of the TGF-beta Family. Cold Spring Harb Perspect Biol 2017;9.
132. Castellone MD, Laukkanen MO. TGF-beta1, WNT, and SHH signaling in tumor progression and in fibrotic diseases. Front Biosci (Schol Ed) 2017;9:31-45.
133. Burgy O, Konigshoff M. The WNT signaling pathways in wound healing and fibrosis. Matrix Biol 2018;68-69:67-80.
134. van Amerongen R, Mikels A, Nusse R. Alternative wnt signaling is initiated by distinct receptors. Sci Signal 2008;1:re9.
135. Aberle H, Bauer A, Stappert J, et al. beta-catenin is a target for the ubiquitin-proteasome pathway. EMBO J 1997;16:3797-804.
136. Piersma B, Bank RA, Boersema M. Signaling in Fibrosis: TGF-beta, WNT, and YAP/TAZ Converge. Front Med (Lausanne) 2015;2:59.
137. Liu C, Li Y, Semenov M, et al. Control of beta-catenin phosphorylation/degradation by a dual-kinase mechanism. Cell 2002;108:837-47.
138. Zeng X, Tamai K, Doble B, et al. A dual-kinase mechanism for Wnt co-receptor phosphorylation and activation. Nature 2005;438:873-7.
139. Davidson G, Wu W, Shen J, et al. Casein kinase 1 gamma couples Wnt receptor activation to cytoplasmic signal transduction. Nature 2005;438:867-72.
140. Li VS, Ng SS, Boersema PJ, et al. Wnt signaling through inhibition of beta-catenin degradation in an intact Axin1 complex. Cell 2012;149:1245-56.
141. Behrens J, von Kries JP, Kuhl M, et al. Functional interaction of beta-catenin with the transcription factor LEF-1. Nature 1996;382:638-42.
142. Molenaar M, van de Wetering M, Oosterwegel M, et al. XTcf-3 transcription factor mediates beta-catenin-induced axis formation in Xenopus embryos. Cell 1996;86:391-9.
143. Duan J, Gherghe C, Liu D, et al. Wnt1/betacatenin injury response activates

the epicardium and cardiac fibroblasts to promote cardiac repair. EMBO J 2012;31:429-42.
144. Lam AP, Gottardi CJ. beta-catenin signaling: a novel mediator of fibrosis and potential therapeutic target. Curr Opin Rheumatol 2011;23:562-7.
145. Akhmetshina A, Palumbo K, Dees C, et al. Activation of canonical Wnt signalling is required for TGF-beta-mediated fibrosis. Nat Commun 2012;3:735.
146. Blyszczuk P, Muller-Edenborn B, Valenta T, et al. Transforming growth factor-beta-dependent Wnt secretion controls myofibroblast formation and myocardial fibrosis progression in experimental autoimmune myocarditis. Eur Heart J 2017;38:1413-1425.
147. Derynck R, Zhang YE. Smad-dependent and Smad-independent pathways in TGF-beta family signalling. Nature 2003;425:577-84.
148. Zhong X, Tu YJ, Li Y, et al. Serum levels of WNT1-inducible signaling pathway protein-1 (WISP-1): a noninvasive biomarker of renal fibrosis in subjects with chronic kidney disease. Am J Transl Res 2017;9:2920-2932.
149. Kendall RT, Feghali-Bostwick CA. Fibroblasts in fibrosis: novel roles and mediators. Front Pharmacol 2014;5:123.
150. Gerdes J, Schwab U, Lemke H, et al. Production of a mouse monoclonal antibody reactive with a human nuclear antigen associated with cell proliferation. Int J Cancer 1983;31:13-20.
151. Stolfi C, Troncone E, Marafini I, et al. Role of TGF-Beta and Smad7 in Gut Inflammation, Fibrosis and Cancer. Biomolecules 2020;11.
152. Rieder F, Kessler S, Sans M, et al. Animal models of intestinal fibrosis: new tools for the understanding of pathogenesis and therapy of human disease. Am J Physiol Gastrointest Liver Physiol 2012;303:G786-801.
153. Sun C, Ma Q, Yin J, et al. WISP-1 induced by mechanical stress contributes to fibrosis and hypertrophy of the ligamentum flavum through Hedgehog-Gli1 signaling. Exp Mol Med 2021;53:1068-1079.
154. Lau LF. Cell surface receptors for CCN proteins. Journal of Cell Communication and Signaling 2016;10:121-127.
155. Jun JI, Kim KH, Lau LF. The matricellular protein CCN1 mediates neutrophil efferocytosis in cutaneous wound healing. Nat Commun 2015;6:7386.
156. Leask A. Signaling in fibrosis: targeting the TGF beta, endothelin-1 and CCN2 axis in scleroderma. Front Biosci (Elite Ed) 2009;1:115-22.
157. Riser BL, Najmabadi F, Perbal B, et al. CCN3/CCN2 regulation and the fibrosis of diabetic renal disease. J Cell Commun Signal 2010;4:39-50.
158. Pivovarova-Ramich O, Loske J, Hornemann S, et al. Hepatic Wnt1 Inducible Signaling Pathway Protein 1 (WISP-1/CCN4) Associates with Markers of Liver Fibrosis in Severe Obesity. Cells 2021;10.
159. Colston JT, de la Rosa SD, Koehler M, et al. Wnt-induced secreted protein-1 is a prohypertrophic and profibrotic growth factor. Am J Physiol Heart Circ Physiol 2007;293:H1839-46.
160. Friedman SL, Sheppard D, Duffield JS, et al. Therapy for fibrotic diseases: nearing the starting line. Sci Transl Med 2013;5:167sr1.
161. Rockey DC, Bell PD, Hill JA. Fibrosis--a common pathway to organ injury and failure. N Engl J Med 2015;372:1138-49.
162. Zeisberg M, Kalluri R. Cellular mechanisms of tissue fibrosis. 1. Common and organ-specific mechanisms associated with tissue fibrosis. Am J Physiol Cell Physiol 2013;304:C216-25.

163. Hinz B, Phan SH, Thannickal VJ, et al. The myofibroblast: one function, multiple origins. Am J Pathol 2007;170:1807-16.
164. Khatun Z, Nishimura N, Kobayashi D, et al. Cesium suppresses fibroblast proliferation and migration. Fukushima J Med Sci 2020;66:97-102.
165. Walraven M, Hinz B. Therapeutic approaches to control tissue repair and fibrosis: Extracellular matrix as a game changer. Matrix Biol 2018;71-72:205-224.
166. Eming SA, Martin P, Tomic-Canic M. Wound repair and regeneration: mechanisms, signaling, and translation. Sci Transl Med 2014;6:265sr6.
167. Pakshir P, Noskovicova N, Lodyga M, et al. The myofibroblast at a glance. J Cell Sci 2020;133.
168. Schuster R, Rockel JS, Kapoor M, et al. The inflammatory speech of fibroblasts. Immunol Rev 2021;302:126-146.
169. Mezzano V, Cabrera D, Vial C, et al. Constitutively activated dystrophic muscle fibroblasts show a paradoxical response to TGF-beta and CTGF/CCN2. J Cell Commun Signal 2007;1:205-17.
170. Komi DEA, Khomtchouk K, Santa Maria PL. A Review of the Contribution of Mast Cells in Wound Healing: Involved Molecular and Cellular Mechanisms. Clin Rev Allergy Immunol 2020;58:298-312.
171. Wang J, Lin S, Brown JM, et al. Novel mechanisms and clinical trial endpoints in intestinal fibrosis. Immunol Rev 2021;302:211-227.
172. Friedrich M, Pohin M, Powrie F. Cytokine Networks in the Pathophysiology of Inflammatory Bowel Disease. Immunity 2019;50:992-1006.
173. Pardali E, Goumans MJ, Ten DP. Signaling by members of the TGF-beta family in vascular morphogenesis and disease. Trends Cell Biol 2010;20:556-67.
174. Eickelberg O, Pansky A, Mussmann R, et al. Transforming growth factor-beta1 induces interleukin-6 expression via activating protein-1 consisting of JunD homodimers in primary human lung fibroblasts. J Biol Chem 1999;274:12933-8.
175. Surendran K, McCaul SP, Simon TC. A role for Wnt-4 in renal fibrosis. Am J Physiol Renal Physiol 2002;282:F431-41.
176. Gordon MD, Nusse R. Wnt signaling: multiple pathways, multiple receptors, and multiple transcription factors. J Biol Chem 2006;281:22429-33.
177. Ackers I, Malgor R. Interrelationship of canonical and non-canonical Wnt signalling pathways in chronic metabolic diseases. Diab Vasc Dis Res 2018;15:3-13.
178. Tan J, Wang Y, Wang S, et al. Label-free quantitative proteomics identifies transforming growth factor beta1 (TGF-beta1) as an inhibitor of adipogenic transformation in OP9-DL1 cells and primary thymic stromal cells. Cell Biosci 2019;9:48.
179. Bayle J, Fitch J, Jacobsen K, et al. Increased expression of Wnt2 and SFRP4 in Tsk mouse skin: role of Wnt signaling in altered dermal fibrillin deposition and systemic sclerosis. J Invest Dermatol 2008;128:871-81.
180. Melkonyan HS, Chang WC, Shapiro JP, et al. SARPs: a family of secreted apoptosis-related proteins. Proc Natl Acad Sci U S A 1997;94:13636-41.
181. Uren A, Reichsman F, Anest V, et al. Secreted frizzled-related protein-1 binds directly to Wingless and is a biphasic modulator of Wnt signaling. J Biol Chem 2000;275:4374-82.
182. Surendran K, Schiavi S, Hruska KA. Wnt-dependent beta-catenin signaling is

activated after unilateral ureteral obstruction, and recombinant secreted frizzled-related protein 4 alters the progression of renal fibrosis. J Am Soc Nephrol 2005;16:2373-84.
183. Wu CL, Tsai HC, Chen ZW, et al. Ras activation mediates WISP-1-induced increases in cell motility and matrix metalloproteinase expression in human osteosarcoma. Cell Signal 2013;25:2812-22.
184. Nivison MP, Meier KE. The role of CCN4/WISP-1 in the cancerous phenotype. Cancer Manag Res 2018;10:2893-2903.
185. Jia S, Qu T, Feng M, et al. Association of Wnt1-inducible signaling pathway protein-1 with the proliferation, migration and invasion in gastric cancer cells. Tumour Biol 2017;39:1010428317699755.
186. Grotendorst GR, Duncan MR. Individual domains of connective tissue growth factor regulate fibroblast proliferation and myofibroblast differentiation. FASEB J 2005;19:729-38.
187. Xu L, Corcoran RB, Welsh JW, et al. WISP-1 is a Wnt-1- and beta-catenin-responsive oncogene. Genes Dev 2000;14:585-95.

Acknowledgement

My deepest gratitude goes out to Prof. Dr. Helmut Friess for accepting me as a medical graduate student at the Technical University of Munich. It is an honor to be able to study at one of the most prestigious universities in the world.

Thank you to my TAC members, Prof. Julia Mayerle and PD Dr. Helga Török, for giving me the opportunity to complete my doctoral degree.

I would like to express my deep and sincere gratitude to my mentor, Philipp-Alexander Neumann, who gave me the opportunity to do research and provided invaluable guidance me throughout this project. Without the support of him, this project would not have been possible. Whenever I was in a difficult and frustrating situation, he was selfless and fearless in helping me. Moreover, I would like to express my gratitude to him for his kind words and thoughtful, detailed comments. Studying and working under his guidance was an honor and privilege. The support he has given me is extremely valuable to me. My sincere thanks go out to him for his friendship, empathy, and sense of humor.

I would like to thank to Dr. Stefan Reischl and Lucia Gampl. It still seems like yesterday that Stafan helped me register with the Foreign Office when I didn't speak German. I would also like to appreciate Lucia for teaching me some experimental techniques.

My sincere thanks also go to Dr. Marie-Christin Weber. During my studies, she provided me with all the guidance, assistance, and expertise I needed.

Also, my thanks and appreciations go out to my colleagues including Annalisa Buck, Chunqiao Li, and the other people who have willingly helped me. I also would like to thank Prof. Klaus-Peter Janssen gave me some study advice.

My parents have spent a significant amount of time, effort, and sacrifice educating and preparing me for the future. I am eternally grateful for their love, devotion, concern, and efforts. I am very grateful for my husband's love, understanding, prayers, and continued support in completing this research project. Additionally, I would like to express my gratitude to my little sister for her support and valuable prayers.

In the End, thanks China Scholarship Council (CSC) for providing me with financial support for my studies and research at Klinikum rechts der Isar Technische

Universtiät München, University of Munich, Germany. It would not have been possible for me to study in Munich without CSC. There are many reasons why I love Munich, not only the lifestyle and way of working, but the scenery, environment, and the most importantly the people.

Affidavit

Affidavit

Shiqian Liu

Surname, first name

Mülhauser str.10a, APP 404

Street

81379, Munich

Zip code, town

Germany

Country

I hereby declare, that the submitted thesis entitled

WNT1-inducible signaling protein-1 induced by TGF-β1 contributes to fibrosis in Crohn's disease

is my own work. I have only used the sources indicated and have not made unauthorised use of services of a third party. Where the work of others has been quoted or reproduced, the source is always given.

I further declare that the dissertation presented here has not been submitted in the same or similar form to any other institution for the purpose of obtaining an academic degree.

Munich,02.11.2022

Place, date

Shiqian Liu

Signature doctoral candidate

Confirmation of congruency

LMU LUDWIG-MAXIMILIANS-UNIVERSITÄT MÜNCHEN

Dean's Office Medical

MMRS

Confirmation of Congruency between Printed and Electronic Version of the Doctoral Thesis

Shiqian Liu

Surname, first name

Mülhauser str.10a, APP 404

Street

81379, Munich

Zip code, town

Germany

Country

I hereby declare, that the submitted thesis entitled

WNT1-inducible signaling protein-1 induced by TGF-β1 contributes to fibrosis in Crohn's diseas

is congruent with the printed version both in content and format.

Munich,02.11.2022

Place, date

Shiqian Liu

Signature doctoral candidate

List of publications

Liu S., Reischl S., Neumann P.-A, et al. Wnt1-inducible signalling protein-1 is associated with intestinal fibrosis in Crohn's disease. United European Gastroenterology. 2020, p0345.